Chapter 5

The PVFP principle

5.1 Introduction

5.1.1 Understanding the PVFP principle with a simple flexible fluidic actuator

As explained before, a flexible fluidic actuator called "the Flexible Microactuator" is presented in [78] and it is suggested that the measurements of the fluid pressure and of the volume of supplied fluid allow to determine and control the position of the actuator and the force it develops. This property, that is referred to as the "Pressure-Volume-Force-Position principle" or "PVFP principle", means being able to determine the displacement of a flexible fluidic actuator and the force it develops without using a displacement sensor or a force sensor [78].

To better understand this principle, let us consider the simple flexible fluidic actuator presented in the left hand side of Fig. 5.1. It is composed of a cylinder whose top is closed by a flexible membrane. The cylinder has a length d and a circular section S of radius R; $S = \pi R^2$. The atmospheric pressure is assumed to be constant and known and the pressure is assumed to be constant.
The outside absolute pressure p_{out} equals the atmospheric pressure p_{atm} and initially, the inner absolute pressure p_{in} is such that $p_{in} = p_{out} = p_{atm}$. When a displacement u is imposed to the piston, the inner pressure p_{in} increases and the membrane deforms and takes the shape of a spherical cap of radius r (see the right hand side of Fig. 5.1). The volume of the spherical cap V_{cap} is completely determined by its radius r and is computed as follows:

$$V_{cap}(r) = \frac{2\pi r^3}{3}\left[1 - \frac{3}{2}(1 - \frac{R^2}{r^2})^{\frac{1}{2}} + \frac{1}{2}(1 - \frac{R^2}{r^2})^{\frac{3}{2}}\right] \tag{5.1}$$

If Poisson's effect is neglected, the membrane surface tension γ is also completely determined by the membrane radius r and is calculated with the following equations:

$$\gamma = \sigma e \tag{5.2}$$

$$\sigma = E_m \frac{\Delta L}{L} \tag{5.3}$$

$$\Delta L = 2r\ \arcsin(\frac{R}{r}) - 2R \tag{5.4}$$

where σ are the stresses in the membrane, e is the membrane thickness, E_m is the membrane Young's modulus, ΔL is the lengthening of the initial membrane length $L = 2R$.

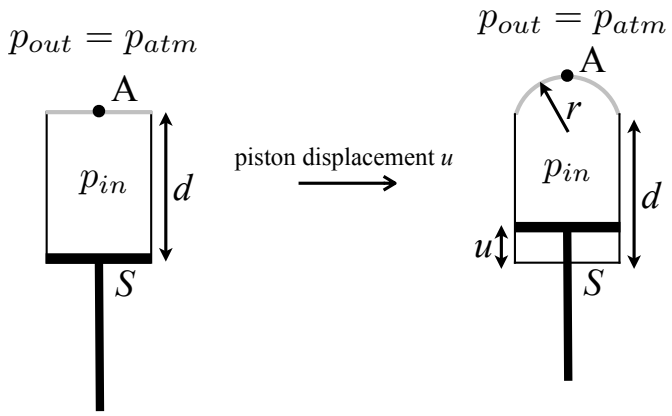

Figure 5.1: Flexible fluidic actuator composed of a cylinder whose top is closed by a flexible membrane. When a displacement u is imposed to the piston, the inner pressure p_{in} increases and the membrane deforms and takes the shape of a spherical cap of radius r. According to the PVFP principle, knowing the values of p_{in} and u allows to determine the vertical displacement of point A and the external pressure p_{ext} applied to the membrane in addition to the atmospheric pressure p_{atm} (see Fig. 5.2).

The volume of fluid supplied to the actuator is considered to be the volume swept by the piston during its displacement; this swept volume is proportional to the piston displacement u and equals Su. Therefore, the piston displacement u will be the variable used for the PVFP principle rather than the swept volume.
According to the PVFP principle, knowing the values of p_{in} and u allows to determine the displacement of the flexible fluidic actuator and the force it develops. For the actuator considered here, the vertical displacement of point A (see Fig 5.1) will be determined and instead of the force developed by the actuator it is the external pressure p_{ext} applied to the membrane (in addition to the atmospheric pressure p_{atm} (see Fig. 5.2)) that will be determined.

First, no external pressure is applied to the membrane and the configuration is that of the right hand side of Fig. 5.1; two cases can be considered:

1. The actuation fluid is incompressible. In this case, the cylinder is initially filled with a volume $V = Sd$ of fluid. When a displacement u is imposed to the piston, the volume of fluid in the cylinder becomes $V' = S(d-u)$ and the volume of the spherical cap equals $V_{cap}(r) = V - V'$. Knowing V_{cap}, equation (5.1) allows to determine the corresponding radius r and knowing r, the vertical displacement of point A can be determined.
   Since r is known, $\gamma(r)$ can be computed with equations (5.2) to (5.4). Concerning the inner pressure p_{in}, it is linked to the outside pressure p_{out}, the membrane radius r and the membrane surface tension γ by the Laplace's equation:

   $$p_{in} - p_{out} = \frac{2\gamma}{r} \tag{5.5}$$

   Since the values of r and γ are known, if the inner pressure p_{in} is measured, the Laplace's equation allows to determine the outside pressure p_{out}. It is thus discovered that $p_{out} = p_{atm}$ and it is deduced that there is no external pressure applied to the membrane.

2. The actuation fluid is compressible. In this case, the cylinder is initially filled with a volume $V = Sd$ of fluid at atmospheric pressure p_{atm}. When a displacement u is

imposed to the piston, the volume of fluid in the cylinder becomes $V' = S(d-u)$. If the pressure p_{in} is measured, r and p_{out} can be determined by the following two equations:

$$p_{atm}Sd = p_{in}(V_{cap}(r) + S(d-u)) \tag{5.6}$$

$$p_{out} = p_{in} - \frac{2\gamma(r)}{r} \tag{5.7}$$

Equation (5.7) is the Laplace's equation while equation (5.6) is the gas law applied to the system whose fluid quantity is constant and assuming that the temperature is constant.
Knowing the value of r, the vertical displacement of point A can be determined and from the value of p_{out}, it can be deduced that there is no external pressure applied to the membrane.

As can be seen, when the membrane is not loaded by an external pressure p_{ext}, the knowledge of the piston displacement u and of the pressure p_{in} allows to determine the displacement of the actuator and to establish that the actuator is not loaded.

Keeping the piston position constant, if an external load is applied to the membrane in the form of an external pressure p_{ext}, the inner pressure p_{in} increases and the radius r of the spherical cap decreases, as represented in Fig. 5.2.

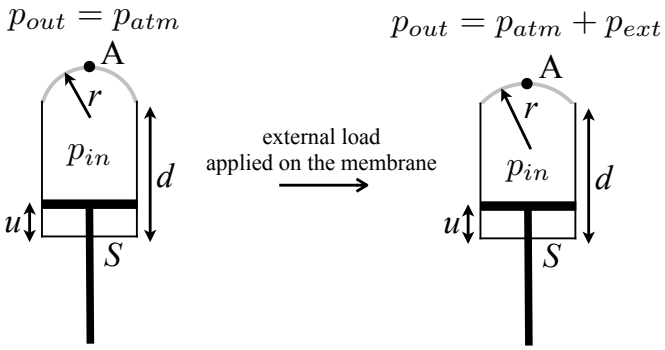

Figure 5.2: Flexible fluidic actuator composed of a cylinder whose top is closed by a flexible membrane. When a displacement u is imposed to the piston, the inner pressure p_{in} increases and the membrane deforms and takes the shape of a spherical cap of radius r. Afterwards, keeping the piston position constant, if an external pressure p_{ext} is applied to the membrane in addition to the atmospheric pressure p_{atm}, the inner pressure p_{in} increases and the radius r of the spherical cap decreases. According to the PVFP principle, knowing the values of p_{in} and u allows to determine the vertical displacement of point A and the external pressure p_{ext}.

Again, two cases can be considered:

1. The actuation fluid is incompressible. In this case, the volume of the cap V_{cap} does not change since the fluid volume V' in the cylinder remains the same. As a consequence, the membrane radius r also remains the same as well as $\gamma(r)$ and as the vertical displacement of point A. If p_{in} is measured, the external pressure p_{ext} can be determined

with the following two equations (the first one being the Laplace's equation):

$$p_{out} = p_{in} - \frac{2\gamma(r)}{r} \tag{5.8}$$

and

$$p_{ext} = p_{out} - p_{atm} \tag{5.9}$$

In fact, since p_{out} increases by an amount p_{ext} while the shape of the membrane does not change, p_{in} increases by the same amount.

2. The actuation fluid is compressible. Since the value of u is known, if p_{in} is measured, the following three equations allow to determine p_{ext} and r (the second equation is the Laplace's equation and the first one is the gas law applied to the system whose fluid quantity is constant and assuming that the temperature is constant) :

$$p_{atm}Sd = p_{in}(V_{cap}(r) + S(d-u)) \tag{5.10}$$

$$p_{out} = p_{in} - \frac{2\gamma(r)}{r} \tag{5.11}$$

$$p_{ext} = p_{out} - p_{atm} \tag{5.12}$$

The vertical displacement of point A can then be determined from the value of r.

As can be seen, when the membrane is loaded, the knowledge of the piston displacement u and of the inner pressure p_{in} allows to determine the displacement of the actuator and the external pressure applied to it.

For the simple actuator discussed in this section, the implementation of the PVFP principle consists thus in the equations that model the behaviour of the actuator and that allow to determine the displacement of the actuator and the external pressure applied to it, on the basis of the values of u and p_{in}.

In the mathematical developments presented in this section, the temperature is considered to be constant as well as the atmospheric pressure. However, in practice, it can happen that the ambient temperature or the atmospheric pressure changes. Let us now consider the effect of those changes on the predictions provided by PVFP principle, in the cases of an incompressible and of a compressible fluid.

1. The actuation fluid is incompressible:

   - If the atmospheric pressure increases by an amount p^*, the absolute outside and inside pressures p_{out} and p_{in} increase by the same amount and the PVFP principle implemented on the actuator perceives this as the application of an external pressure $p_{ext} = p^*$. To get rid of the influence of an atmospheric pressure change, a gauge pressure sensor could be used to measure p_{in} or the atmospheric pressure could be measured and updated, if necessary, in the implementation of the PVFP principle (i.e. in equation (5.9)).
   - If the ambient temperature increases by a small amount such that the volume of fluid does not change (no expansion), it will have no influence on the results provided by the PVFP principle, i.e. the predictions of the actuator displacement and of the external pressure applied to the membrane will not be distorted.

2. The actuation fluid is compressible.

   - If the atmospheric pressure increases by an amount p^*, the absolute outside pressure p_{out} increases by the same amount, the radius r of the spherical cap decreases as well as the vertical displacement of point A and p_{in} increases but not by the same amount as p_{out}. Indeed, if p_{out} and p_{in} increased by the same amount, equation (5.7) would lead to an unchanged radius r while in practice r decreases. The PVFP principle implemented on the actuator perceives the change of the atmospheric pressure as the application of an external pressure $p_{ext} = p^*$. As already said, the change of the atmospheric pressure has lead to a change of the vertical displacement of point A but the prediction of the PVFP principle, according to which $p_{ext} = p^*$, can be used to compensate this change and to restore the displacement of point A. The PVFP principle does not allow to distinguish a change of the atmospheric pressure from the application of a real external pressure p_{ext}; to be able to do so, it is necessary to measure the atmospheric pressure.
     The atmospheric pressure needs thus to be measured and updated in the implementation of the PVFP principle (i.e. in equation (5.12)) and its effect on the displacement of point A needs to be compensated if it is non-negligible.
   - If the ambient temperature increases, the volume of fluid expands in the actuator. Since the volume V' in the cylinder does not change because the piston position is imposed, the volume V_{cap} of the spherical cap increases as well as the vertical displacement of point A. The inner pressure p_{in} increases and the PVFP principle implemented on the actuator perceives this change as the application of an external pressure $p_{ext} = p^*$ that would have decreased the displacement of point A. Hence, the prediction of the PVFP principle, according to which $p_{ext} = p^*$, can not be used to compensate the change in the displacement of point A due to the temperature increase; indeed, doing so would lead to a further increase of the displacement of this point! The temperature needs thus to be measured and taken into account in the implementation of the PVFP principle and its effect on the displacement of point A needs to be compensated.

In conclusion, for the simple actuator considered here, the PVFP principle is applicable with an incompressible or a compressible actuation fluid. Besides, if an incompressible actuation fluid and a gauge pressure sensor (to measure p_{in}) are used, the predictions provided by the PVFP principle implemented on the actuator will not be influenced by the changes of the atmospheric pressure and of the temperature.

5.1.2 Implementing the PVFP principle on the Pneumatic Balloon Actuator

The Pneumatic Balloon Actuator (PBA) has been chosen to study the PVFP principle. This actuator is described in Section 4.2 and is installed on the test bench described in Sections 3.5 and 4.3.
Fig. 5.3 is a schematic representation of the PBA linked to the cylinder of the test bench. The actuation fluid is air. When a displacement u is imposed to the piston, the inner pressure p_{in} increases and the PBA inflates and its free end A moves upwards. The vertical and horizontal displacements of this point are Δy_0 and Δx_0, respectively. Afterwards, keeping the piston position constant, if a weight w is hung from the PBA free end, the inner pressure p_{in} increases by an amount Δp and the displacements Δy and Δx of the PBA free end decrease. According to the PVFP principle, knowing the values of p_{in} and u allows to determine the displacements of point A and the value of the weight w.

As explained before, the pressure variation Δp due to the loading of the PBA with a weight is measured with another sensor than the inner pressure p due to the piston displacement (p is the gauge pressure corresponding to the absolute pressure p_{in}).

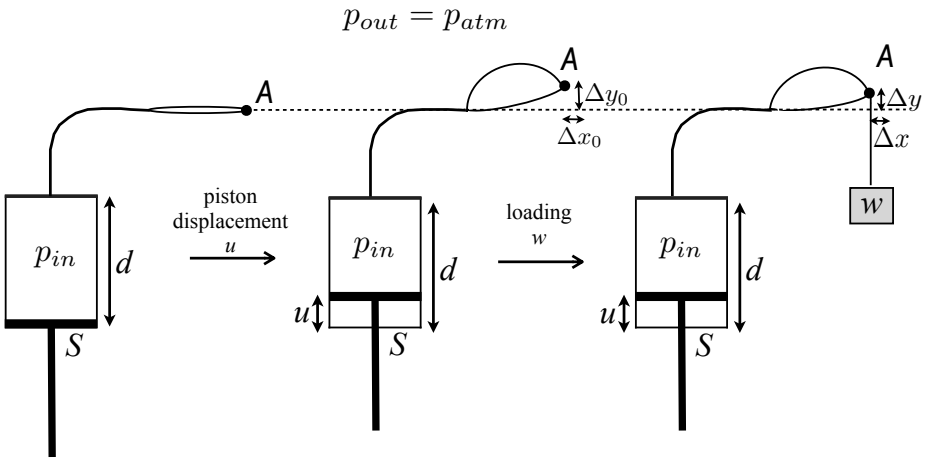

Figure 5.3: Pneumatic Balloon Actuator (PBA) linked to the cylinder of the test bench. The actuation fluid is air. When a displacement u is imposed to the piston, the inner pressure p_{in} increases and the PBA inflates and its free end A moves upwards. The vertical and horizontal displacements of this point are Δy_0 and Δx_0, respectively. Afterwards, keeping the piston position constant, if a weight w is hung from the PBA free end, the inner pressure p_{in} increases and the displacements Δy and Δx of the PBA free end decrease. According to the PVFP principle, knowing the values of p_{in} and u allows to determine the displacements of point A and the value of the weight w.

To implement the PVFP principle on the PBA, experiments are performed in order to establish experimental models of the PBA; this is done is Section 5.2.1 and the following experimental models are established:

- $p = p(u)$
- $\Delta x_0 = \Delta x_0(u)$
- $\Delta y_0 = \Delta y_0(u)$
- $\Delta p = \Delta p(u, w)$
- $\Delta x = \Delta x(u, w)$
- $\Delta y = \Delta y(u, w)$

Afterwards, in Section 5.2.2, the PVFP principle is used to predict the PBA displacements Δx and Δy and the load w attached from its free end, on the basis of the measurements of u and p. In summary, this is done as follows:

- If it is known that the PBA is not loaded (i.e. no pressure variation Δp is measured while the piston position is kept constant), the measurement of the piston displacement u allows to determine the inner pressure p and the PBA displacements Δx_0 and Δy_0, thanks to the first three experimental models.

- If it is known that the PBA is loaded (i.e. a pressure variation Δp is measured while the piston position is kept constant), the measurements of the piston displacement u and of the pressure variation Δp allow to determine the PBA displacements Δx and Δy as well as the load w, thanks to the last three experimental models.

Finally, Section 5.2.3 studies the hysteresis of the PBA and Section 5.3 discusses the relevance of the PVFP principle and its practical implementation.

5.2 Experimental study of the PVFP principle

5.2.1 Establishing experimental models of the PBA's behaviour

The aim of the experiments is to establish the following relationships:

- $p = p(u)$
- $\Delta x_0 = \Delta x_0(u)$
- $\Delta y_0 = \Delta y_0(u)$
- $\Delta p = \Delta p(u, w)$
- $\Delta x = \Delta x(u, w)$
- $\Delta y = \Delta y(u, w)$

To do so, a design of experiments (DOE) has been established with the help of the Design-Expert 8 software [11]. Since there are two factors, u and w, a response surface design has been chosen and more precisely a central composite design (CCD). A CCD has been selected because quadratic models can be established with it and because previous experiments revealed that the relationships listed above can be approached by polynomials not higher than quadratic ones. A CCD will lead to models giving very good predictions in the middle of the experimental space $u - w$; it is a factorial design to which center and axial points are added to estimate the quadratic terms. The DOE proposed by the software counts thirteen experiments, i.e. combinations (u, w) of the factors u and w, that have to be performed in a random order. These experiments are represented in the experimental space $u - w$, in Fig. 5.4.

As can be seen,

- five experiments repeat the same combination (u, w) which is placed at the center of the experimental space; these replicated center points are used to estimate pure error for the lack of fit test. Lack of fit indicates how well the chosen model fits the data. Moreover, these center points are used to estimate the quadratic terms.

- four experiments are combinations (u, w) placed on the horizontal or vertical axis passing through the center point of the experimental space; these axial points are also used to estimate the quadratic terms.

- four experiments are combinations (u, w) which are not placed on the horizontal nor the vertical axis passing through the center point of the experimental space; these experiments correspond to the factorial design associated with the two factors u and w.

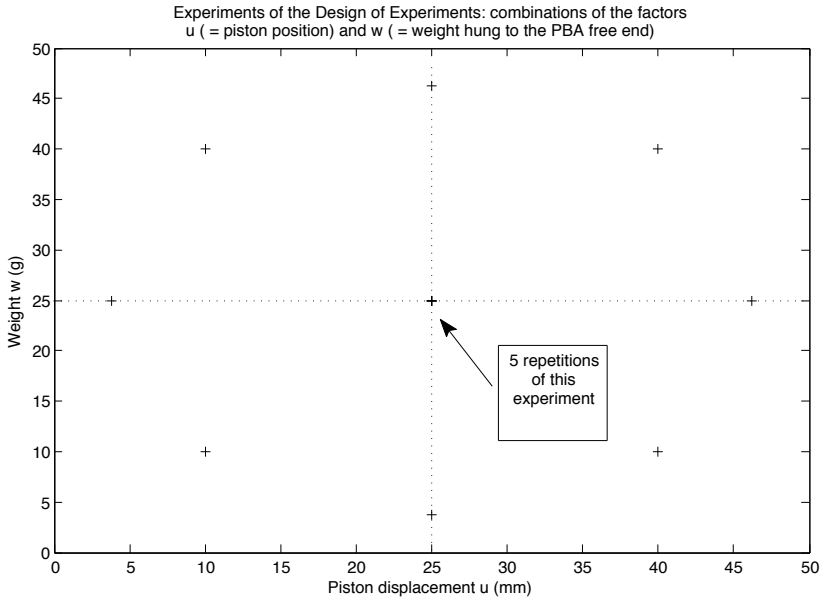

Figure 5.4: Experiments of the Design of Experiments (DOE) performed to establish the following relationships for the studied PBA: $p = p(u)$, $\Delta x_0 = \Delta x_0(u)$, $\Delta y_0 = \Delta y_0(u)$, $\Delta p = \Delta p(u, w)$, $\Delta x = \Delta x(u, w)$, $\Delta y = \Delta y(u, w)$. The chosen DOE is a central composite design of thirteen experiments: five central points, four axial points and four other points corresponding to the factorial design associated to the two factors u (= piston displacement) and w (= weight hung to the PBA free end).

- the DOE requires to perform specific experiments. However, in practice, if the linear motor is asked to perform a given piston displacement u^*, it will perform a displacement u' close to u^* but not equal to u^*; the difference between u^* and u' can be as large as 1 mm. Besides, some weights were not feasible, such as 3.79 g or 46.21 g, and were replaced by 4 g and 46 g, respectively. Hence, the DOE has been updated to take these differences into account.

- the practical range of u is $[4\text{ mm}, 46\text{ mm}]$. The lower value has been chosen because the corresponding position of the PBA is quite well repeatable. Indeed, the PBA needs to be a little bit pressurized to have a repeatable position. The upper value allows to pressurize the PBA without exceeding its maximum admitted pressure of 0.3 bar. The position of the PBA has been measured for $u = 4.46$ mm and it has been considered to be the PBA rest position, i.e. no X- or Y-displacements, since then.

For each experiment, the required piston displacement u has been reached. Then the pressure p and the X- and Y-displacements Δx_0 and Δy_0 have been measured. Afterwards, the specified weight w has been hung from the PBA free end and the pressure variation Δp, the X- and Y-displacements Δx and Δy have been measured. The weight has then been removed before performing the next experiment.
Fig. 5.5 to 5.11 present the results of this DOE. The crosses and circles indicate the experiments (some points may be superimposed) while the lines and surfaces represent the experimental models established on the basis of these experiments.

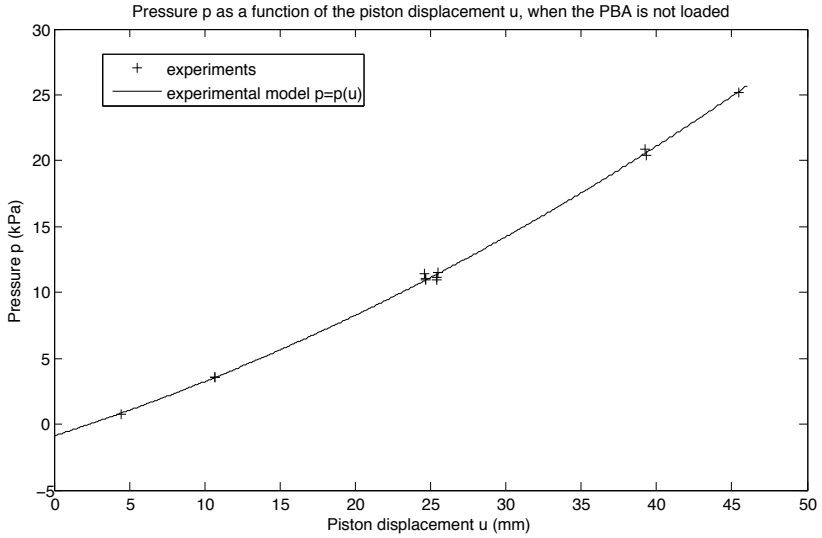

Figure 5.5: Pressure p as a function of the piston displacement u, when the PBA is not loaded. The crosses represent the thirteen performed experiments (some points may be superimposed) and the line is the experimental model $p = p(u)$ established on the basis of these experiments.

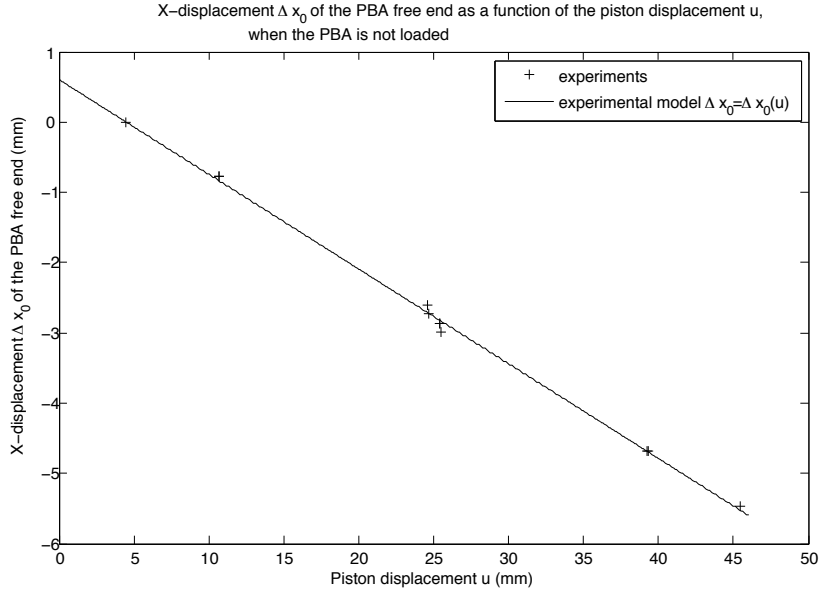

Figure 5.6: X-displacement Δx_0 of the PBA free end as a function of the piston displacement u, when the PBA is not loaded. The crosses represent the thirteen performed experiments (some points may be superimposed) and the line is the experimental model $\Delta x_0 = \Delta x_0(u)$ established on the basis of these experiments.

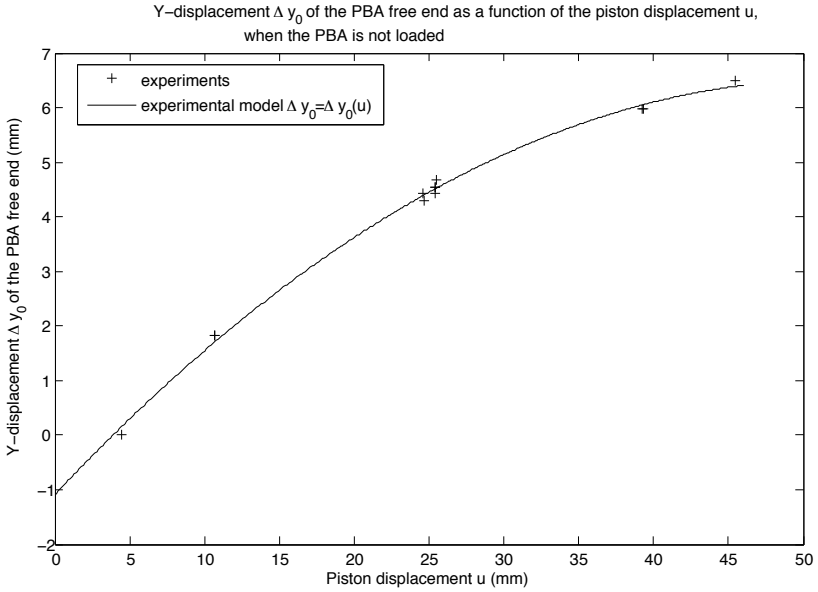

Figure 5.7: Y-displacement Δy_0 of the PBA free end as a function of the piston displacement u, when the PBA is not loaded. The crosses represent the thirteen performed experiments (some points may be superimposed) and the line is the experimental model $\Delta y_0 = \Delta y_0(u)$ established on the basis of these experiments.

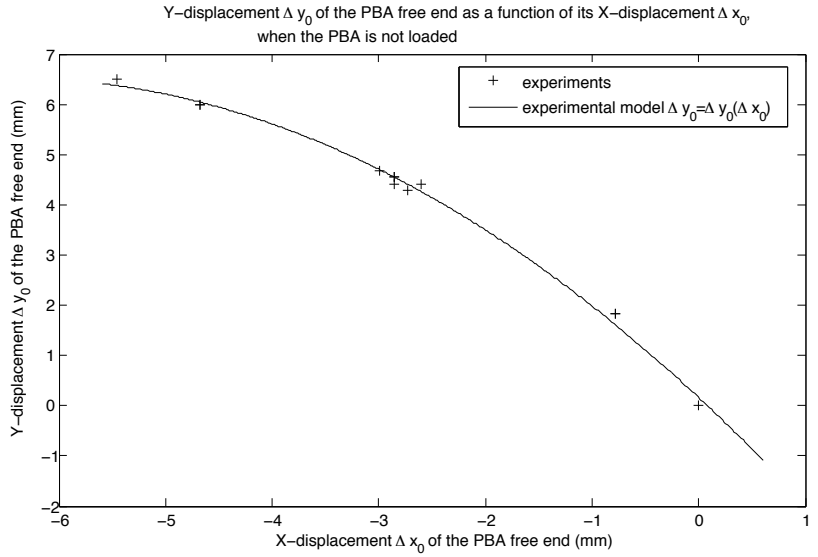

Figure 5.8: Y-displacement Δy_0 of the PBA free end as a function of its X-displacement Δx_0, when the PBA is not loaded. The crosses represent the thirteen performed experiments (some points may be superimposed) and the line is the experimental model $\Delta y_0 = \Delta y_0(\Delta x_0)$ established on the basis of these experiments.

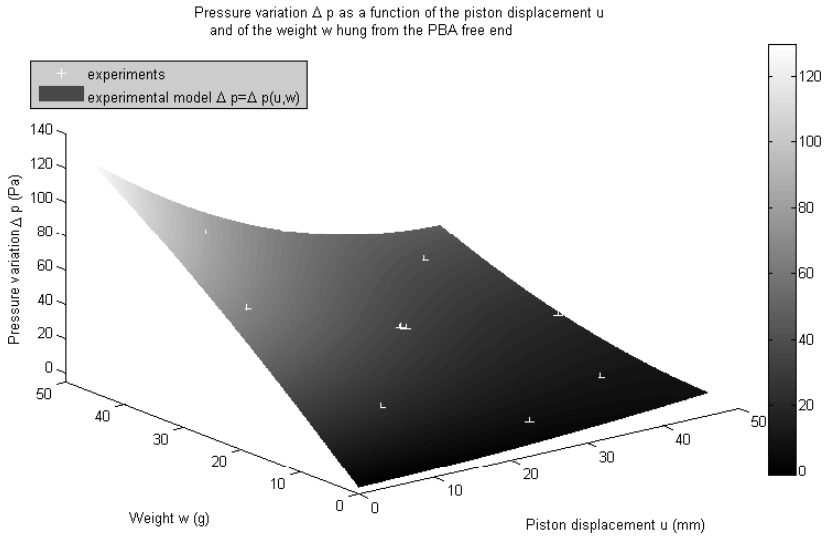

Figure 5.9: Pressure variation Δp as a function of the piston displacement u and of the weight w hung from the PBA free end. The crosses represent the thirteen performed experiments (some points may be superimposed) and the surface is the experimental model $\Delta p = \Delta p(u, w)$ established on the basis of these experiments.

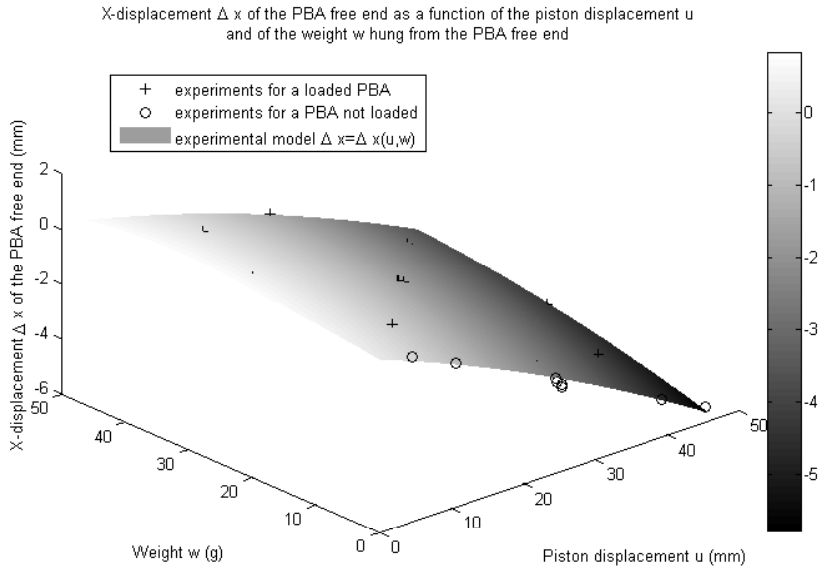

Figure 5.10: X-displacement Δx of the PBA free end as a function of the piston displacement u and of the weight w hung from the PBA free end. The crosses represent the thirteen performed experiments (some points may be superimposed) and the surface is the experimental model $\Delta x = \Delta x(u, w)$ established on the basis of these experiments. The circles represent the experiments performed for a PBA not loaded (these are the experiments presented in Fig. 5.6).

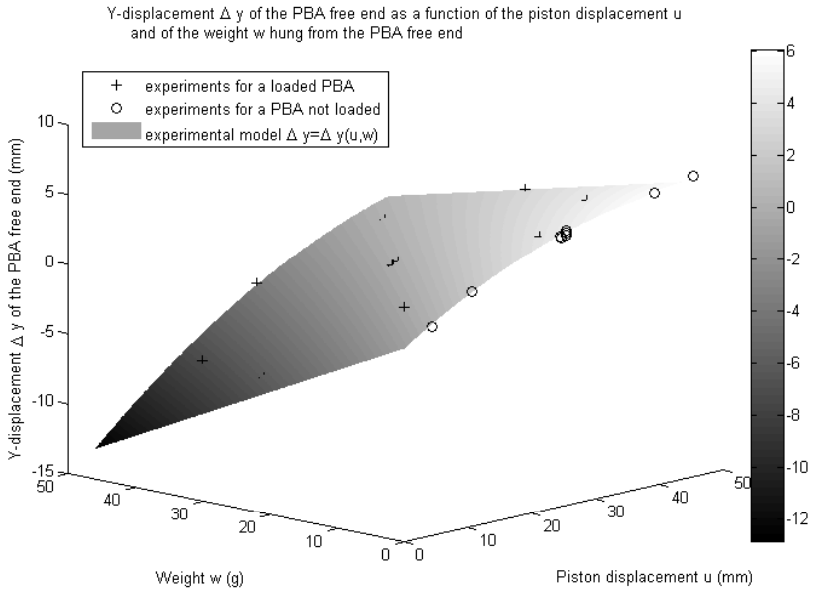

Figure 5.11: Y-displacement Δy of the PBA free end as a function of the piston displacement u and of the weight w hung from the PBA free end. The crosses represent the thirteen performed experiments (some points may be superimposed) and the surface is the experimental model $\Delta y = \Delta y(u, w)$ established on the basis of these experiments. The circles represent the experiments performed for a PBA not loaded (these are the experiments presented in Fig. 5.7).

The equations of the experimental models are the following (the values of the coefficients are given in Table 5.1):

$$p = c_1 + c_2 u + c_3 u^2 \tag{5.13}$$

$$\Delta x_0 = d_1 + d_2 u \tag{5.14}$$

$$\Delta y_0 = f_1 + f_2 u + f_3 u^2 \tag{5.15}$$

$$\Delta p = b_1 + b_2 u + b_3 w + b_4 u\ w + b_5 u^2 + b_6 w^2 + b_7 u^2 w + b_8 u\ w^2 \tag{5.16}$$

$$\Delta x = g_1 + g_2 u + g_3 w + g_4 u\ w + g_5 u^2 + g_6 w^2 \tag{5.17}$$

$$\Delta y = a_1 + a_2 u + a_3 w + a_4 u\ w + a_5 u^2 \tag{5.18}$$

Coefficients	Coefficients
$a_1 = -1.155$	$c_1 = -0.8826$
$a_2 = 0.3100$	$c_2 = 0.3656$
$a_3 = -0.2545$	$c_3 = 4.606\ 10^{-3}$
$a_4 = 2.887\ 10^{-3}$	$d_1 = 0.6049$
$a_5 = -3.327\ 10^{-3}$	$d_2 = -0.1348$
$b_1 = -1.135$	$f_1 = -1.089$
$b_2 = 5.067\ 10^{-2}$	$f_2 = 0.2913$
$b_3 = 3.313$	$f_3 = -2.787\ 10^{-3}$
$b_4 = -0.1048$	$g_1 = 0.2557$
$b_5 = 3.146\ 10^{-3}$	$g_2 = -9.785\ 10^{-2}$
$b_6 = -1.016\ 10^{-2}$	$g_3 = 3.598\ 10^{-2}$
$b_7 = 7.688\ 10^{-4}$	$g_4 = 7.567\ 10^{-4}$
$b_8 = 5.469\ 10^{-4}$	$g_5 = -7.232\ 10^{-4}$
	$g_6 = -5.561\ 10^{-4}$

Table 5.1: Values of the coefficients of the experimental models

As can be seen,

- the pressure p has a quadratic evolution with respect to the piston displacement u and if u is increased, p increases.
- the X-displacement Δx_0 has a linear evolution with respect to the piston displacement u. If u is increased, the PBA free end moves upwards, Δx_0 increases in absolute value (Δx_0 is negative and decreases).
- the Y-displacement Δy_0 has a quadratic evolution with respect to the piston displacement u. If u is increased, the PBA free end moves upwards and Δy_0 increases.
- the pressure variation Δp has a cubic evolution with respect to the piston displacement u and to the weight w hung from the PBA free end. For a given piston displacement u, if the weight w is increased, the pressure variation Δp increases. On the other hand, for a given weight w, if the piston displacement u is increased, the pressure variation Δp decreases.
  In practice, when the PBA is not loaded ($w = 0$), the pressure variation Δp equals zero but the experimental model forecasts a pressure variation Δp up to 8 Pa, as can be seen in Fig. 5.9 and 5.12. On the other hand, in practice, when there is no pressure variation ($\Delta p = 0$), it means that the PBA is not loaded ($w = 0$) but the experimental model forecasts a non-zero weight, apart from one value of u, as can be seen in Fig. 5.9 and 5.13.

- the X- and Y-displacements Δx and Δy have both a quadratic evolution with respect to the piston displacement u and to the weight w hung from the PBA free end. For a given piston displacement u, if the weight w is increased, the PBA free end moves downwards and Δy decreases. On the other hand, for a given weight w, if the piston displacement u is increased, the PBA free end moves upwards and Δy increases.

In Fig. 5.14 and 5.15, it is interesting to notice that the experimental models $\Delta x_0 = \Delta x_0(u)$ and $\Delta y_0 = \Delta y_0(u)$ are quite similar to the experimental models $\Delta x = \Delta x(u, w)$ and $\Delta y = \Delta y(u, w)$, respectively, when there is no load ($w = 0$). As a consequence, the models of Δx and Δy can be rewritten as follows:

$$\Delta x(u, w) \approx \Delta x_0(u) + \Delta x_w(u, w) \tag{5.19}$$

with

$$\Delta x_w(u, w) = (g_3 + g_4 u)w + g_6 w^2 \tag{5.20}$$

$$\Delta y(u, w) \approx \Delta y_0(u) + \Delta y_w(u, w) \tag{5.21}$$

with

$$\Delta y_w(u, w) = (a_3 + a_4 u)w \tag{5.22}$$

With these expressions, one can clearly see that Δx and Δy are the results of two contributions:

1. $\Delta x_0(u)$ and $\Delta y_0(u)$: these first contributions are linked to the piston displacement u when the PBA is not loaded; $\Delta x|_{u,w=0} = \Delta x_0(u)$ and $\Delta y|_{u,w=0} = \Delta y_0(u)$.

2. $\Delta x_w(u, w)$ and $\Delta y_w(u, w)$: this contribution is linked to the weight w hung from the PBA free end but also to the piston displacement u. Hence, if a given weight is hung at the PBA free end, the corresponding X- and Y-displacements Δx_w and Δy_w will be different for two different piston displacements. The expression 5.22 of $\Delta y_w(u, w)$ indicates that $\Delta y_w(u, w)$ has a linear evolution with respect to the weight w, whose slope depends on the piston displacement u. In other words, $\Delta y_w(u, w)$ evolves as a spring with respect to the weight, whose stiffness depends on the piston displacement: the higher the piston displacement, the stiffer the spring.

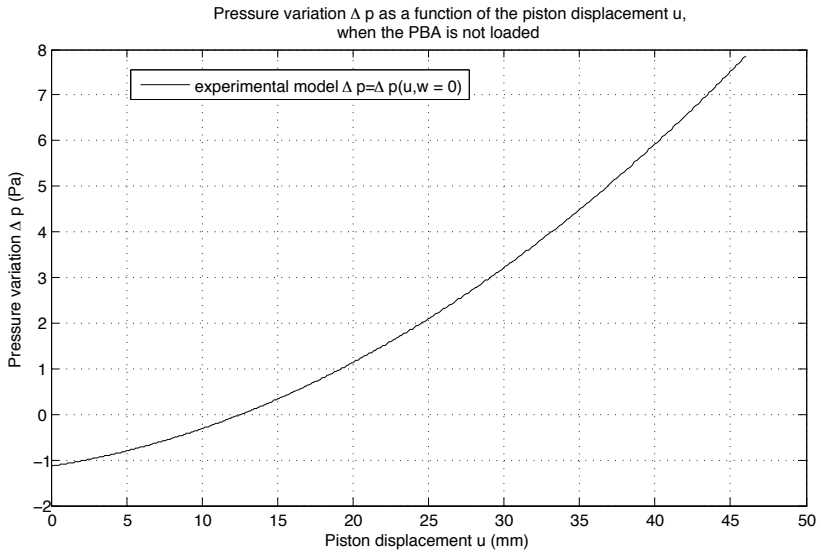

Figure 5.12: Pressure variation Δp as a function of the piston displacement u, when the PBA is not loaded. The solid line is the experimental model $\Delta p = \Delta p(u, w)$, when there is no load ($w = 0$). In practice, Δp equals zero when the PBA is not loaded but the experimental model forecasts a value up to 8 Pa.

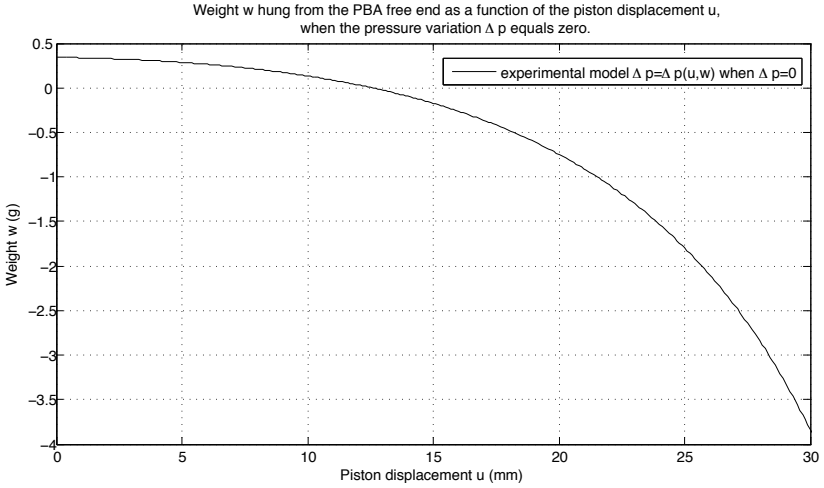

Figure 5.13: Weight w hung from the PBA free end as a function of the piston displacement u, when the pressure variation Δp equals zero. The solid line is the experimental model $\Delta p = \Delta p(u, w)$ for $\Delta p = 0$. In practice, when there is no pressure variation, it means that the PBA is not loaded but the experimental model forecasts a non-zero weight, apart from one value of u. u does not range above 30 mm because above this value the experimental model keeps on forecasting negative weights and even weights having an imaginary part.

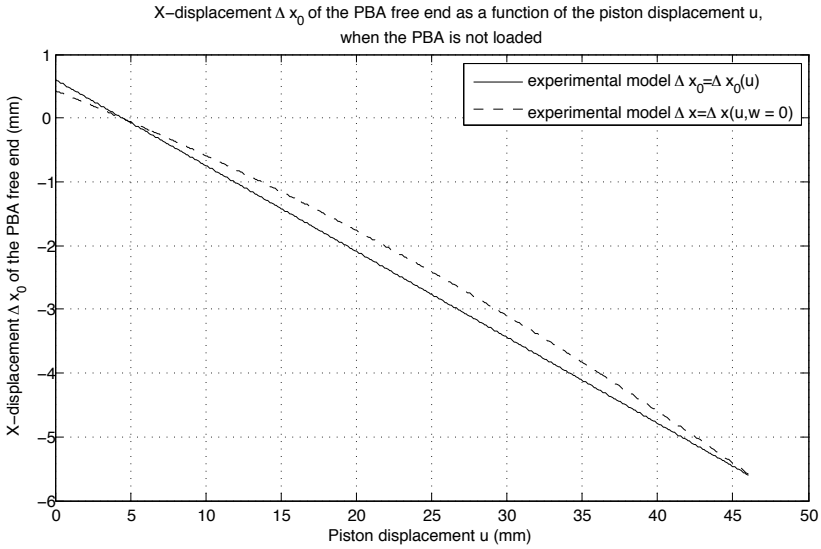

Figure 5.14: X-displacement Δx_0 of the PBA free end as a function of the piston displacement u. The solid line is the experimental model $\Delta x_0 = \Delta x_0(u)$ while the dashed line is the experimental model $\Delta x = \Delta x(u, w)$ when the PBA is not loaded ($w = 0$). As can be seen, both models are quite similar.

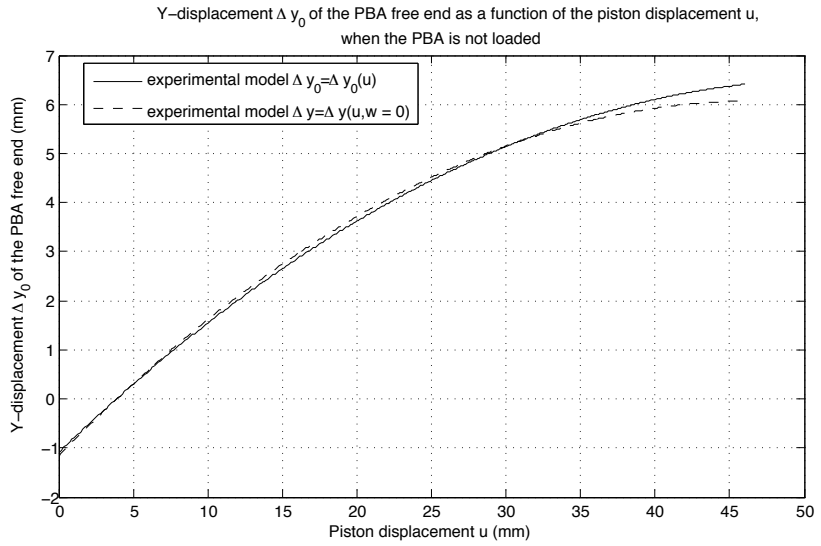

Figure 5.15: Y-displacement Δy_0 of the PBA free end as a function of the piston displacement u. The solid line is the experimental model $\Delta y_0 = \Delta y_0(u)$ while the dashed line is the experimental model $\Delta y = \Delta y(u, w)$ when the PBA is not loaded ($w = 0$). As can be seen, both models are quite similar.

5.2.2 Application of the PVFP principle: using the PBA as a sensor

Now that the experimental models of the PBA's behaviour have been established, they can be used to implement the PVFP principle. As presented in Fig. 5.16, the goal is to use the measurements of the piston displacement u and of the pressure variation Δp together with the experimental models to predict the values of the actuator displacements and of the weight attached from its end.

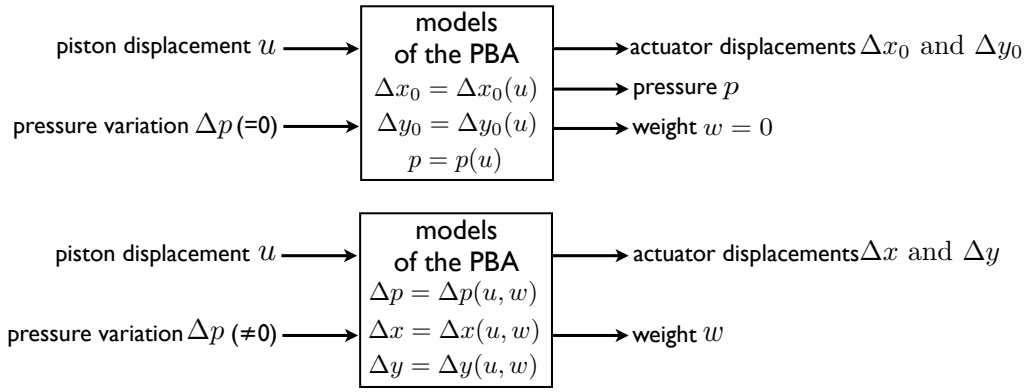

Figure 5.16: Representation of the implementation of the PVFP principle: on the basis of the measurements of the the piston displacement u and of the pressure variation Δp, the experimental models of the PBA are used to predict the values of the actuator displacements and of the weight attached to it.

1. If there is no pressure variation while the piston position is kept constant, i.e. $\Delta p = 0$, it means that the actuator has not been loaded with a weight. Hence, it can be predicted that $w = 0$; it is better to say directly that $w = 0$ than to use the experimental model $\Delta p = \Delta p(u, w)$ to predict the weight w because, as explained before, this model will not predict a zero value for the weight if $\Delta p = 0$ (see Fig. 5.13). The experimental models $p = p(u)$, $\Delta x_0 = \Delta x_0(u)$ and $\Delta y_0 = \Delta y_0(u)$ (see expressions 5.13, 5.14 and 5.15 and Fig. 5.5, 5.6 and 5.7) can then been used to predict the values p^*, Δx_0^* and Δy_0^* of p, Δx_0 and Δy_0 on the basis of the piston displacement measurement u

2. If there is a pressure variation while the piston position is kept constant, i.e. $\Delta p \neq 0$, it means that the actuator has been loaded with a weight w. The experimental models $\Delta p = \Delta p(u, w)$, $\Delta x = \Delta x(u, w)$ and $\Delta y = \Delta y(u, w)$ can then been used to predict the values w^*, Δx^* and Δy^* of w, Δx and Δy on the basis of the piston displacement and pressure variation measurements u and Δp.
   This is presented in Fig. 5.17, 5.18 and 5.19. First, both measurements u and Δp are used together with the experimental model $\Delta p = \Delta p(u, w)$ to predict the value w^* of the weight w that loads the PBA. Indeed, as can be seen in Fig. 5.17, for a given piston displacement u and a given pressure variation Δp, there is only one possible prediction for the weight. Afterwards, the piston displacement measurement u and the predicted value of the weight w^* are used together with the experimental models $\Delta x = \Delta x(u, w)$ and $\Delta y = \Delta y(u, w)$ to predict the values Δx^* and Δy^* of Δx and Δy. As can be seen in Fig. 5.18 and 5.19, there is only one possible prediction for Δx or Δy, for a given piston displacement u and a given weight w^*.

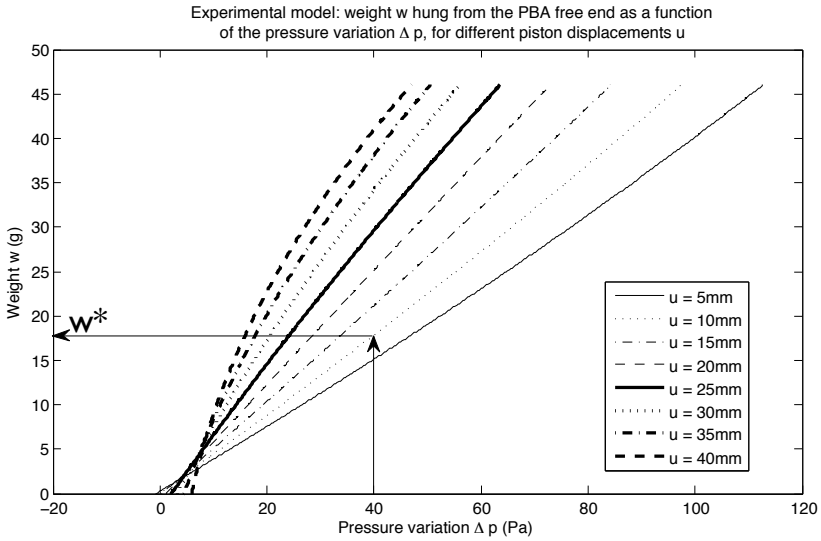

Figure 5.17: Experimental model $\Delta p = \Delta p(u, w)$, for a loaded PBA: the weight w hung from the PBA free end is presented with respect to the pressure variation Δp, for different values of the piston displacement u. On the basis of the measurements u and Δp, this model can predict the value w^* of the weight that loads the PBA. Indeed, as can be seen in the figure, for a given u and a given Δp, there is only one possible prediction w^* for the weight. For example, if $u = 10$ mm and $\Delta p = 40$ Pa, the experimental model predicts that $w^* = 17.8522$ g.

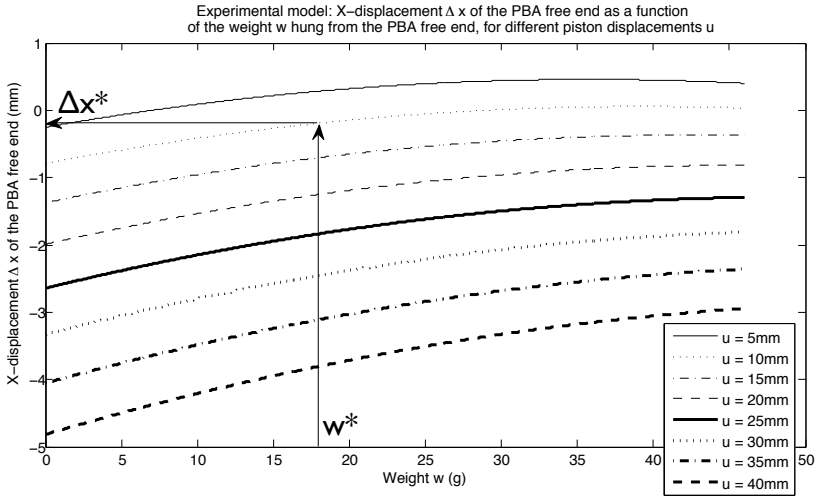

Figure 5.18: Experimental model $\Delta x = \Delta x(u, w)$, for a loaded PBA: the X-displacement Δx of the PBA free end is presented with respect to the weight w, for different values of the piston displacement u. On the basis of the measurement u and the prediction w^*, this model can predict the value Δx^* of the X-displacement of the PBA. Indeed, as can be seen in the figure, for a given u and a given w^*, there is only one possible prediction Δx^* for the X-displacement. For example, if $u = 10$ mm and $w^* = 17.8522$ g, the experimental model predicts that $\Delta x^* = -0.1949$ mm.

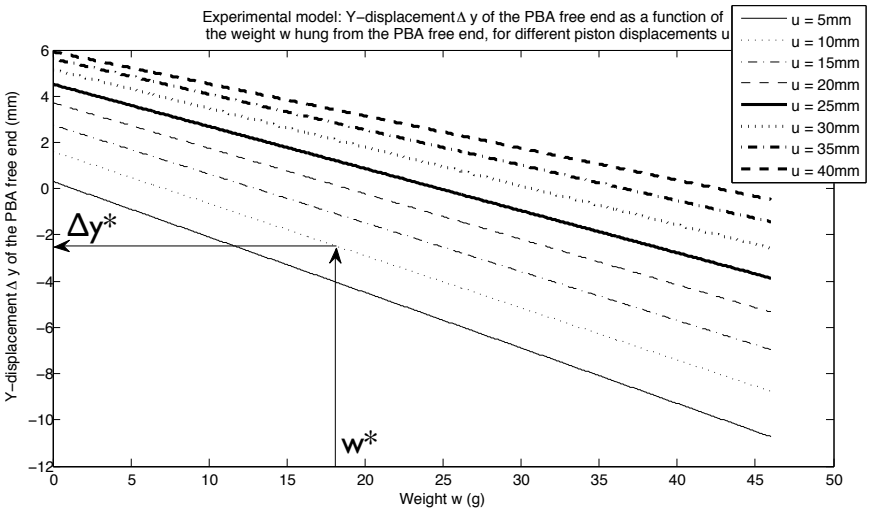

Figure 5.19: Experimental model $\Delta y = \Delta y(u, w)$, for a loaded PBA: the Y-displacement Δy of the PBA free end is presented with respect to the weight w, for different values of the piston displacement u. On the basis of the measurement u and the prediction w^*, this model can predict the value Δy^* of the Y-displacement of the PBA. Indeed, as can be seen in the figure, for a given u and a given w^*, there is only one possible prediction Δy^* for the Y-displacement. For example, if $u = 10$ mm and $w^* = 17.8522$ g, the experimental model predicts that $\Delta y^* = -2.4154$ mm.

To test the implementation of the PVFP principle on the studied PBA, the experiments summarized in Table 5.2 have been performed:

Experiment number	Piston displacement (mm)	Weight (g)	Measurements
1	15.61	0	p, Δx_0, Δy_0
2	15.61	35	Δp, Δx, Δy
3	15.61	15	Δp, Δx, Δy
4	15.61	20	Δp, Δx, Δy
5	19.71	0	p, Δx_0, Δy_0
6	19.71	35	Δp, Δx, Δy
7	19.71	15	Δp, Δx, Δy
8	19.71	20	Δp, Δx, Δy
9	34.36	0	p, Δx_0, Δy_0
10	34.36	35	Δp, Δx, Δy
11	34.36	15	Δp, Δx, Δy
12	34.36	20	Δp, Δx, Δy

Table 5.2: Experiments performed to test the implementation of the PVFP principle on the studied PBA. For each experiment, the table indicates for the chosen piston displacement u and weight w as well as the made measurements.

It has to be underlined that for each experiment, the specified weight w has been hung from the PBA free end and then removed before the next experiment is performed. For each experiment, the predictions have been made as explained above.

The experiments no. 1, 5 and 9 and corresponding predictions are presented in Fig. 5.20, 5.21 and 5.22; the PBA is not loaded for these experiments.
As can be seen,

- in Fig. 5.20, the measured pressures p are very close to the predicted ones p^*.
- in Fig. 5.21, the measured X-displacements Δx_0 are larger in absolute value than the predicted ones Δx_0^*.
- in Fig. 5.22, the measured Y-displacements Δy_0 are larger than the predicted ones Δy_0^*.

Fig. 5.23 and 5.24 present the absolute and relative errors, respectively, on the predictions of p, Δx_0 and Δy_0. These errors are summarized in Table 5.3. The absolute and relative errors on a given prediction are computed as follows:

$$absolute\ error = measured\ value - prediction \tag{5.23}$$

$$relative\ error = 100(measured\ value - prediction)/measured\ value \tag{5.24}$$

Parameter	Absolute error	Relative error
p	max 0.24 kPa	max 3.30% of the measured value
Δx_0	max 0.26 mm in absolute value	max 11.26% of the measured value
Δy_0	max 0.73 mm	max 20.83% of the measured value

Table 5.3: Absolute and relative errors on the predictions of p, Δx_0 and Δy_0.

For the other experiments (i.e. experiments no. 2, 3, 4, 6, 7, 8, 10, 11 and 12), the PBA is loaded; they are presented, together with the corresponding predictions, in Fig. 5.25, 5.26, 5.27 and 5.28. As can be seen in Fig. 5.26, the measured X-displacements Δx are larger in absolute value than the predicted ones Δx^*.
Fig. 5.29 and 5.30 present the absolute and relative errors, respectively, on the predictions of w, Δx and Δy. These errors are summarized in Table 5.4.

Parameter	Absolute error	Relative error
w	max 1.85 g in absolute value	max 10.68% of the measured value, in absolute value
Δx	max 0.38 mm in absolute value	max 28.81% of the measured value
Δy	max 0.55 mm in absolute value	experiment no. 3: 61.70% of the measured value experiment no. 10: 139.40% of the measured value other experiments: max 20.28% of the measured value, in absolute value

Table 5.4: Absolute and relative errors on the predictions of w, Δx and Δy.

As can be seen in Fig. 5.30 and Table 5.4, experiments no. 3 and 10 have a relative error on the prediction of Δy that equals to 61.70% and 139.40% of the measured value, respectively; on the other hand, the other experiments have a relative error on the prediction of Δy of maximum 20.28% of the measured value. To understand these two outliers, one has to look at the corresponding absolute errors (see Table 5.5). As can be seen, these absolute errors have reasonable values compared to the rest of the experiments but they are of the same order of magnitude than the corresponding Δy measurements and this explains the high values of the relative errors. The relative error on the prediction of Δy of experiment

no. 8 is not represented in Fig. 5.30 because it is infinite; indeed, the Δy measurement of this experiment equals zero (see Table 5.5).
Remark: In Fig. 5.28, it is interesting to notice that the curve $\Delta y = \Delta y(\Delta x)$ travelled by the PBA free end when it is loaded is different according to the piston displacement u.

Experiment number	Δy measurement	Δy^* prediction	Absolute error	Relative error
3	-0.39 mm	-0.1494 mm	-0.2406 mm	61.70% of the measured value
8	0 mm	-0.13 mm	0.13 mm	∞
10	0.26 mm	-0.1024 mm	0.3624 mm	139.40% of the measured value

Table 5.5: Table summarizing the Δy measurement, the Δy^* prediction, the absolute and relative errors on the prediction of Δy, for the experiments no. 3, 8 and 10. Experiments no. 3 and 10 have very large relative errors on the prediction of Δy (in comparison with the other experiments) because their absolute errors are of the same order of magnitude than their Δy measurements. Experiment no. 8 has an infinite relative error on the prediction of Δy because its Δy measurement equals zero.

In conclusion, this section has proved experimentally that the PVFP principle can be applied to the PBA. The quality of the predictions provided by the PVFP principle implemented on the PBA has to be evaluated with respect to an application. Hence, the predictions presented here can be sufficient for an application where qualitative results are needed, such as being able to compare loads applied to the PBA and having a coarse idea of the resulting position of the PBA free end. For an application requiring more accurate results, the predictions presented here may be insufficient.
The errors on the measurements (see Table 4.1) have not been taken into account while computing the absolute and relative errors of Tables 5.3 and 5.4, but if they were, they would increase the maximum errors that can be obtained.
The errors between the predictions and the corresponding measurements may be due to the fact that the fluidic circuit presents some leakages, that the experimental models are not perfect, that the PBA presents some hysteresis as will be shown in the Section 5.2.3 and that there are errors on the measurements due to the sensors.

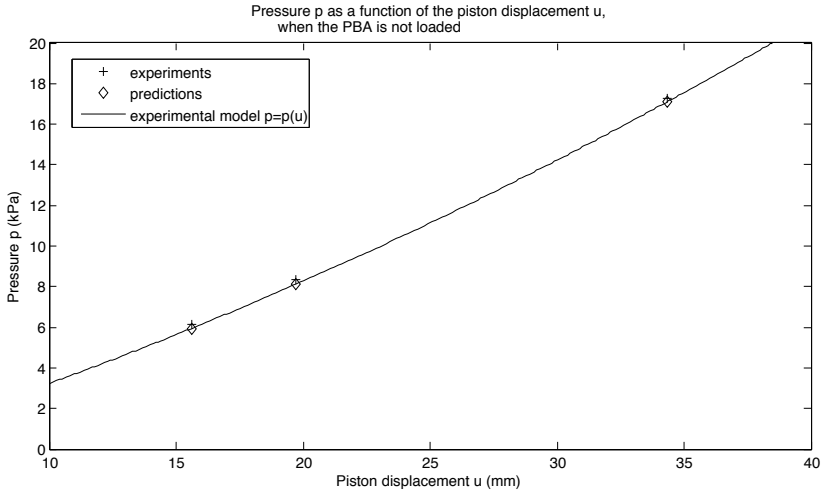

Figure 5.20: Pressure p as a function of the piston displacement u, when the PBA is not loaded: The crosses represent the experiments no. 1, 5 and 9 of Table 5.2 while the diamonds represent the corresponding predictions. Indeed, for the given piston displacements u, the PVFP principle implemented on the studied PBA predicts pressures p^* thanks to the experimental model $p = p(u)$. The predictions are represented by the diamonds. The solid line is the experimental model $p = p(u)$. As can be seen, the measured pressures p are very close to the predicted ones p^*.

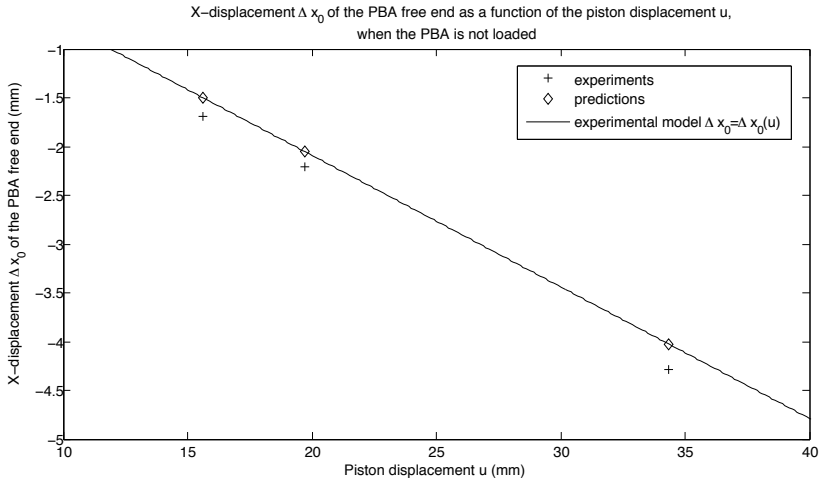

Figure 5.21: X-displacement Δx_0 of the PBA free end as a function of the piston displacement u, when the PBA is not loaded: The crosses represent the experiments no. 1, 5 and 9 of Table 5.2 while the diamonds represent the corresponding predictions. Indeed, for the given piston displacements u, the PVFP principle implemented on the studied PBA predicts X-displacements Δx_0^* thanks to the experimental model $\Delta x_0 = \Delta x_0(u)$. The predictions are represented by the diamonds. The solid line is the experimental model $\Delta x_0 = \Delta x_0(u)$. As can be seen, the measured X-displacements Δx_0 are larger in absolute value than the predicted ones Δx_0^*.

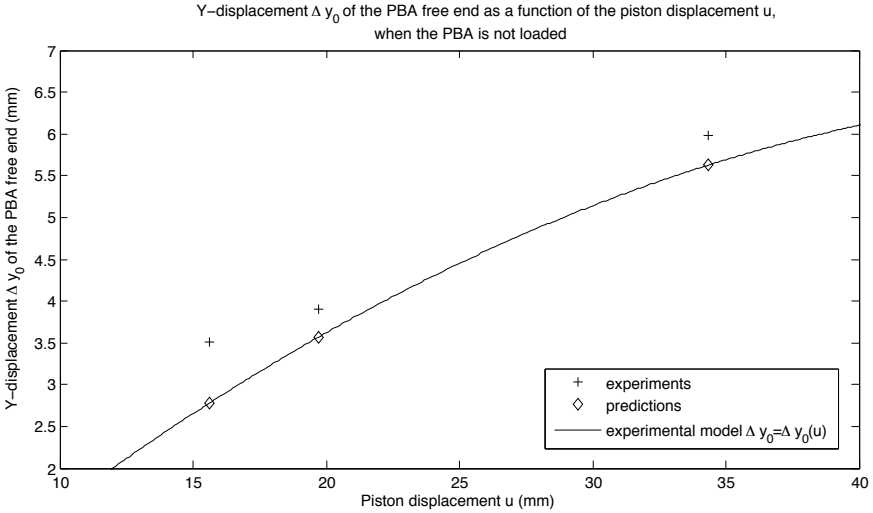

Figure 5.22: Y-displacement Δy_0 of the PBA free end as a function of the piston displacement u, when the PBA is not loaded: The crosses represent the experiments no. 1, 5 and 9 of Table 5.2 while the diamonds represent the corresponding predictions. Indeed, for the given piston displacements u, the PVFP principle implemented on the studied PBA predicts Y-displacements Δy_0^* thanks to the experimental model $\Delta y_0 = \Delta y_0(u)$. The predictions are represented by the diamonds. The solid line is the experimental model $\Delta y_0 = \Delta y_0(u)$. As can be seen, the measured Y-displacements Δy_0 are larger than the predicted ones Δy_0^*.

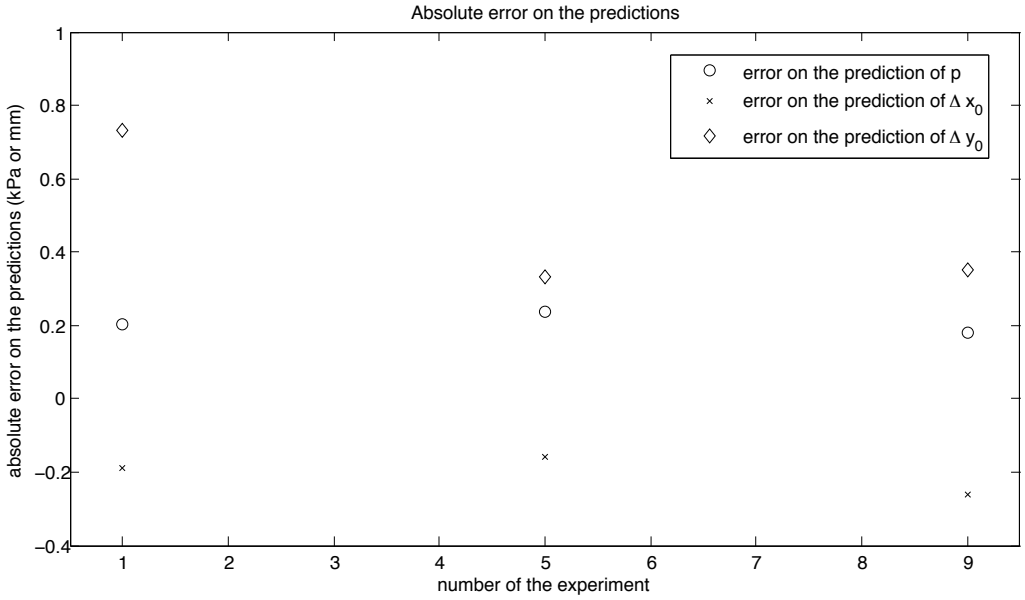

Figure 5.23: Absolute errors on the predictions of p, Δx_0 and Δy_0 for the experiments no. 1, 5 and 9 of Table 5.2. For the given piston displacements u, the PVFP principle implemented on the studied PBA predicts pressures p^*, X-displacements Δx_0^* and Y-displacements Δy_0^* thanks to the experimental models $p = p(u)$, $\Delta x_0 = \Delta x_0(u)$ and $\Delta y_0 = \Delta y_0(u)$. According to the parameter (p, Δx_0 or Δy_0), the error is expressed in kPa or mm.

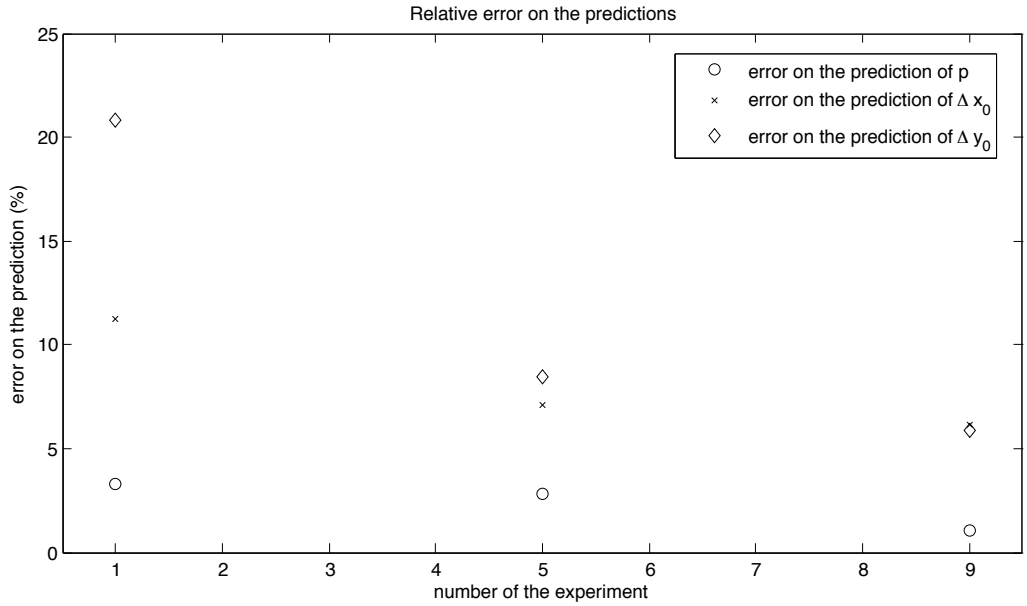

Figure 5.24: Relative errors on the predictions of p, Δx_0 and Δy_0 for the experiments no. 1, 5 and 9 of Table 5.2. For the given piston displacements u, the PVFP principle implemented on the studied PBA predicts pressures p^*, X-displacements Δx_0^* and Y-displacements Δy_0^* thanks to the experimental models $p = p(u)$, $\Delta x_0 = \Delta x_0(u)$ and $\Delta y_0 = \Delta y_0(u)$.

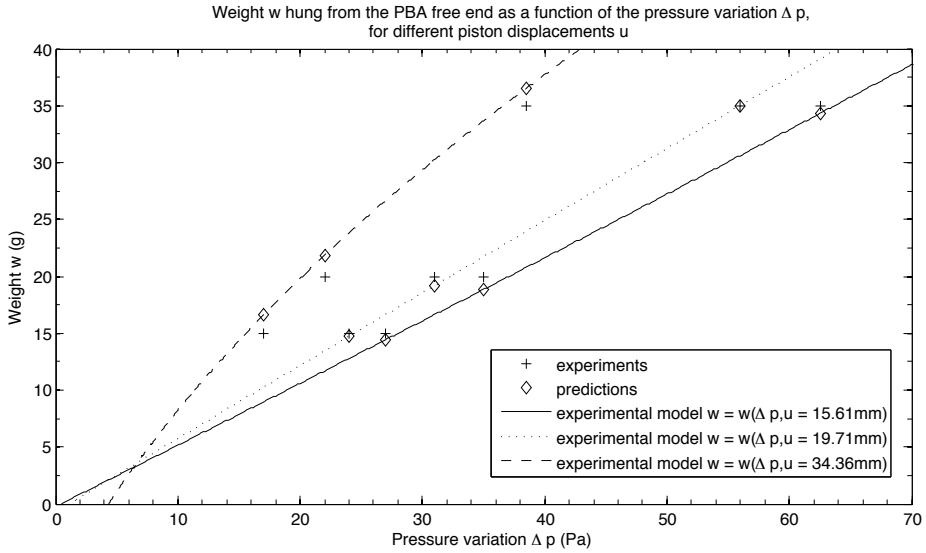

Figure 5.25: Weight w attached to the PBA free end as a function of the pressure variation Δp, for different piston displacements u: The crosses represent the experiments no. 2, 3, 4, 6, 7, 8, 10, 11 and 12 of Table 5.2 while the diamonds represent the corresponding predictions. Indeed, for the given piston displacements u and the given pressure variations Δp, the PVFP principle implemented on the studied PBA predicts weights w^* thanks to the experimental model $\Delta p = \Delta p(u, w)$.

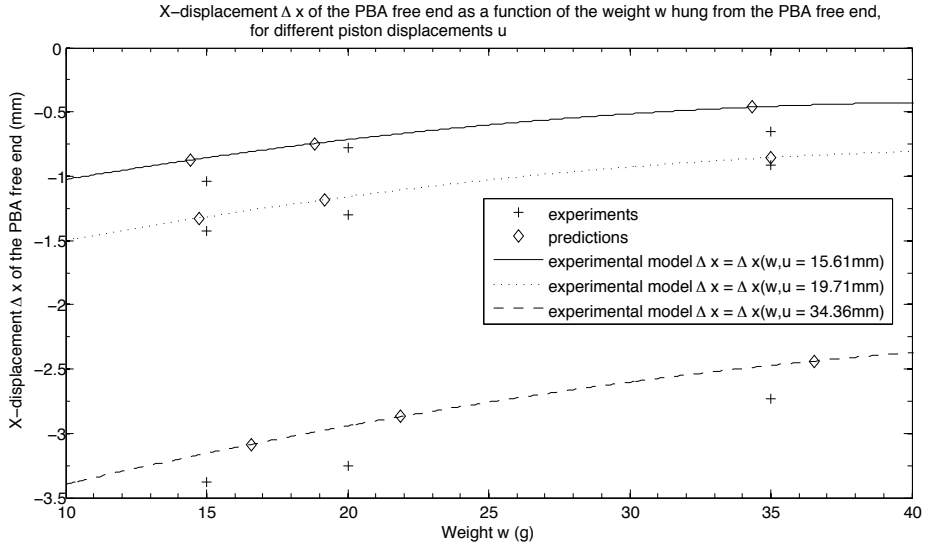

Figure 5.26: X-displacement Δx of the PBA free end as a function of the weight w hung from the PBA free end, for different piston displacements u: The crosses represent the experiments no. 2, 3, 4, 6, 7, 8, 10, 11 and 12 of Table 5.2 while the diamonds represent the corresponding predictions. Indeed, for the given piston displacements u and the predicted weights w^*, the PVFP principle implemented on the studied PBA predicts X-displacements Δx^* thanks to the experimental model $\Delta x = \Delta x(u, w)$. As can be seen, the measured X-displacements Δx are larger in absolute value than the predicted ones Δx^*.

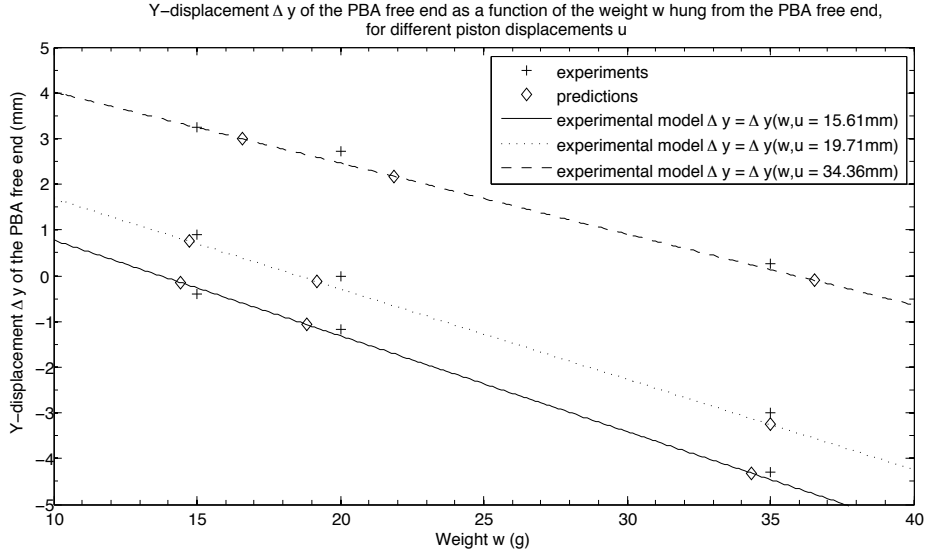

Figure 5.27: Y-displacement Δy of the PBA free end as a function of the weight w hung from the PBA free end, for different piston displacements u: The crosses represent the experiments no. 2, 3, 4, 6, 7, 8, 10, 11 and 12 of Table 5.2 while the diamonds represent the corresponding predictions. Indeed, for the given piston displacements u and the predicted weights w^*, the PVFP principle implemented on the studied PBA predicts Y-displacements Δy^* thanks to the experimental model $\Delta y = \Delta y(u, w)$.

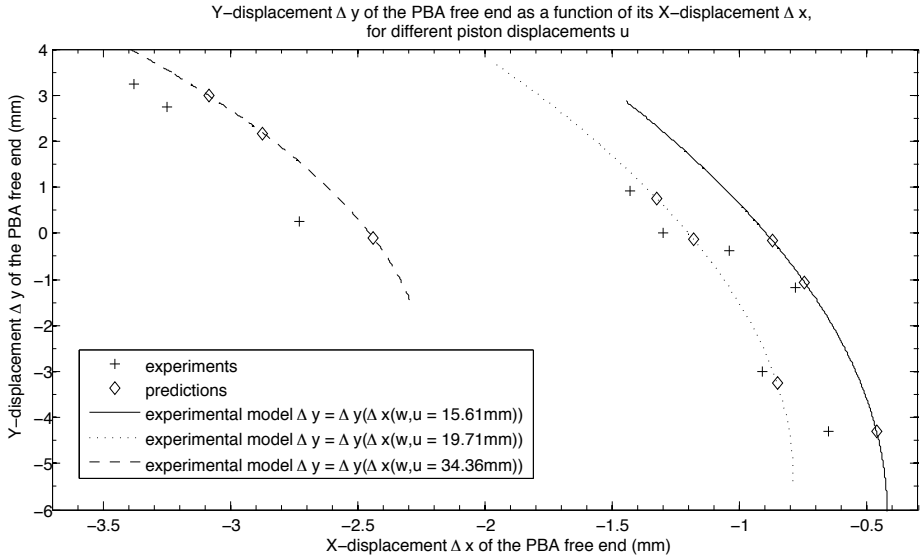

Figure 5.28: Y-displacement Δy of the PBA free end as a function of its X-displacement Δx, for different piston displacements u: The crosses represent the experiments no. 2, 3, 4, 6, 7, 8, 10, 11 and 12 of Table 5.2 while the diamonds represent the corresponding predictions. Indeed, for the given piston displacements u and the predicted weights w^*, the PVFP principle implemented on the studied PBA predicts X-displacements Δx^* and Y-displacements Δy^* thanks to the experimental models $\Delta x = \Delta x(u, w)$ and $\Delta y = \Delta y(u, w)$.

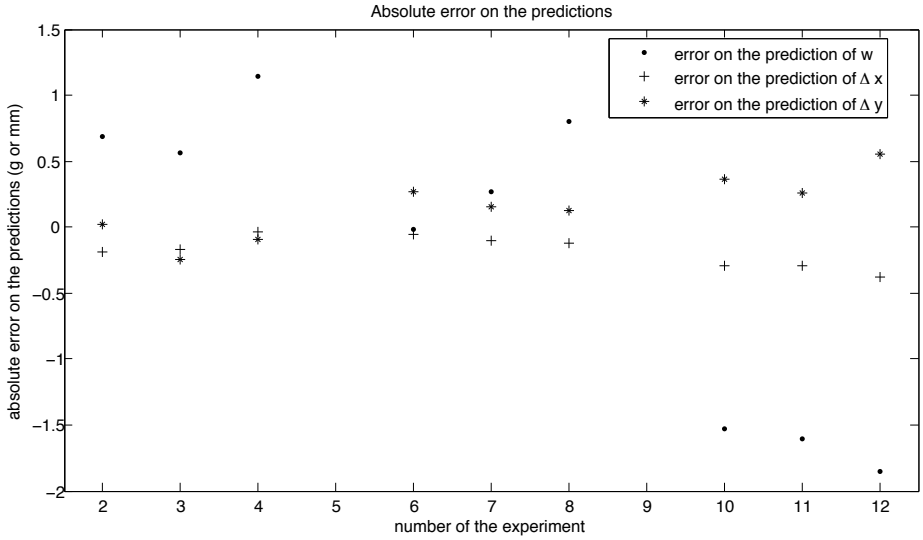

Figure 5.29: Absolute errors on the predictions of Δp, Δx and Δy for the experiments no. 2, 3, 4, 6, 7, 8, 10, 11 and 12 of Table 5.2. For the given piston displacements u and the given pressure variations Δp, the PVFP principle implemented on the studied PBA predicts weights w^*, X-displacements Δx^* and Y-displacements Δy^* thanks to the experimental models $\Delta p = \Delta p(u, w)$, $\Delta x = \Delta x(u, w)$ and $\Delta y = \Delta y(u, w)$. According to the parameter (w, Δx or Δy), the error is expressed in g or mm.

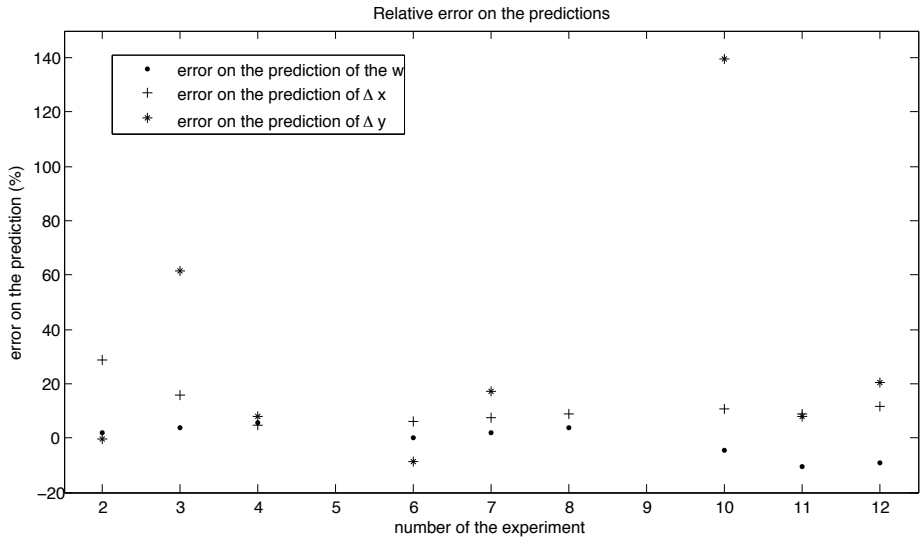

Figure 5.30: Relative errors on the predictions of Δp, Δx and Δy for the experiments no. 2, 3, 4, 6, 7, 8, 10, 11 and 12 of Table 5.2. For the given piston displacements u and the given pressure variations Δp, the PVFP principle implemented on the studied PBA predicts weights w^*, X-displacements Δx^* and Y-displacements Δy^* thanks to the experimental models $\Delta p = \Delta p(u, w)$, $\Delta x = \Delta x(u, w)$ and $\Delta y = \Delta y(u, w)$.

5.2.3 Study of the hysteresis of the PBA

Models have been established in order to implement the PVFP principle on the studied PBA. These models have been built on the basis of a DOE counting thirteen experiments performed in a random order. This means that if PBA variables (i.e. p, Δx_0, Δy_0, Δp, Δx or Δy) present hysteresis with respect to the piston displacement u or with respect to the weights w attached to the PBA, this hysteresis is not properly modeled by the experimental models. A study has thus been made to determine whether some of the PBA variables show hysteresis with respect to u and/or w. First, the hysteresis with respect to the piston displacement u has been investigated. Three hysteresis loops have been performed as follows:

1. first hysteresis loop: 1) $u = 5$ mm, 2) $u = 15$ mm, 3) $u = 5$ mm
2. second hysteresis loop: 1) $u = 5$ mm, 2) $u = 15$ mm, 3) $u = 25$ mm, 4) $u = 15$ mm, 5) $u = 5$ mm
3. third hysteresis loop: 1) $u = 5$ mm, 2) $u = 15$ mm, 3) $u = 25$ mm, 4) $u = 35$ mm, 5) $u = 25$ mm, 6) $u = 15$ mm, 7) $u = 5$ mm

For each piston displacement, the pressure p and the X- and Y-displacements Δx_0 and Δy_0 have been measured and the PBA has not been loaded. The results of this hysteresis study are presented in Fig. 5.31 to 5.38.

Remark: Let us consider that the error on two measurements equals $\pm$ s. If both measurements are spaced out by a difference smaller than $2s$, there is a probability that the exact measurements corresponding to them are equal. On the other hand, if both measurements are spaced out by a difference larger than $2s$, it is sure that the exact measurements corresponding to them are different. Table 4.1 summarizes the errors on the measurements.

Concerning the results of the hysteresis study:

- As can be seen in Fig. 5.31 and 5.32, the pressure p presents nearly no hysteresis with respect to the piston displacement u.
- As can be seen in Fig. 5.33 and 5.34, it can be concluded that the X-displacement Δx_0 presents a hysteresis with respect to the piston displacement u: when comparing the increasing and decreasing phases of u, the maximum difference in X-displacement that has been measured is about 0.26 mm (the accuracy on the measurement of Δx_0 equals ± 0.13 mm)
- As can be seen in Fig. 5.35 and 5.36, it can be concluded that the Y-displacement Δy_0 presents a hysteresis with respect to the piston displacement u: when comparing the increasing and decreasing phases of u, the maximum difference in Y-displacement that has been measured is larger than 0.26 mm (the accuracy on the measurement of Δy_0 equals ± 0.13 mm).

The experimental models $p = p(u)$, $\Delta x_0 = \Delta x_0(u)$ and $\Delta y_0 = \Delta y_0(u)$ have been established with a DOE whose experiments are performed in a random order. As a consequence, the hysteresis of Δx_0 and Δy_0 with respect to the piston displacement u is not properly modeled by these experimental models. On the contrary, it is drowned into these models.

Afterwards, the hysteresis with respect to the weight w attached from the PBA free end has been investigated. Again, three hysteresis loops have been performed, but not the same day as the previous hysteresis study:

1. first hysteresis loop: 1) $w = 0$ g, 2) $w = 10$ g, 3) $w = 0$ g

2. second hysteresis loop: 1) $w = 0$ g, 2) $w = 10$ g, 3) $w = 20$ g, 4) $w = 10$ g, 5) $w = 0$ g
3. third hysteresis loop: 1) $w = 0$ g, 2) $w = 10$ g, 3) $w = 20$ g, 4) $w = 40$ g, 5) $w = 20$ g, 6) $w = 10$ g, 7) $w = 0$ g

During these three loops, the piston displacement has been kept constant and equal to $u = 24.61$ mm. Contrary to the experiments performed before (see Sections 5.2.1 and 5.2.2), for these hysteresis loops, the weight w is progressively increased or decreased from an experiment to the next one. For example, the second hysteresis loop is performed as follows:

- first experiment: no weight is attached to the PBA free end. $\Delta p = 0$ and the X- and Y-displacements Δx and Δy are measured. Since the PBA is not loaded, $\Delta x = \Delta x_0$ and $\Delta y = \Delta y_0$.
- second experiment: a weight of 10 g is attached to the PBA free end and Δp, Δx and Δy are measured.
- third experiment: a second weight of 10 g is added to reach a total weight of 20 g and Δp, Δx and Δy are measured.
- fourth experiment: 10 g are removed to leave a 10 g weight hanging at the PBA free end. Δp, Δx and Δy are measured.
- fifth experiment: finally, the last 10 g are removed. Δp, Δx and Δy are measured. Since the PBA is no more loaded, $\Delta x = \Delta x_0$ and $\Delta y = \Delta y_0$.

The results of this hysteresis study are presented in Fig. 5.39 to 5.46:

- As can be seen in Fig. 5.39 and 5.40, it can be concluded that Δp presents nearly no hysteresis with respect to the weight w. Indeed, 0.5 Pa is the maximum difference in pressure variation measured during the hysteresis loops, when comparing the increasing and decreasing phases of w (the accuracy on a pressure variation measurement is $\leq \pm 4$ Pa).
- As can be seen in Fig. 5.41 and 5.42, it can be concluded that Δx presents a hysteresis with respect to the weight w: when comparing the increasing and decreasing phases of w, the maximum difference in X-displacement that has been measured is smaller than 0.26 mm (the accuracy on the measurement of Δx equals ± 0.13 mm).
- As can be seen in Fig. 5.44, it can be concluded that Δy presents a hysteresis with respect to the weight w: when comparing the increasing and decreasing phases of w during the third hysteresis loop, the maximum difference in Y-displacement that has been measured is larger than 0.26 mm. In Fig. 5.43, the maximum difference in Y-displacement that has measured during the first and second hysteresis loops is smaller than 0.26 mm (the accuracy on the measurement of Δy equals ± 0.13 mm).

The hysteresis of Δx and Δy with respect to the weight w is not taken into account in the experimental models $\Delta x = \Delta x(u, w)$ and $\Delta y = \Delta y(u, w)$ established previously.

In conclusion, to properly model the hysteresis of Δx_0 and Δy_0 with respect to the piston displacement u and the hysteresis of Δx and Δy with respect to the weight w, new experimental models should be established. To do so, more hysteresis loops as the ones presented above should be performed to better understand the hysteresis behaviour of the variables. Besides, complementary hysteresis tests have to be performed because the variables Δp, Δx and Δy depend on w but also on u; however, only their hysteresis with respect to w has been studied. To study the hysteresis of these variables with respect to u, the following tests can be performed:

- a given weight w is attached at the PBA free and Δx and Δy are measured while u performs cycles (one cycle = increasing phase + decreasing phase). This allows to study the hysteresis of Δx and Δy with respect to u.
- while u performs cycles, the same weight is hung and then removed from the PBA free end and Δp is measured. This allows to study the hysteresis of Δp with respect to u.

Before modeling the hysteresis, it has to be assessed whether this hysteresis is problematic or not with respect to the targeted application. Indeed, for a given application, the hysteresis of the variables may be small enough to be negligible; in this case, there is no need to model the hysteresis. On the other hand, for another application, the hysteresis of the variables may be too large to be ignored; in this case, it has to be modeled properly.

As can be seen in Fig. 5.31 and Fig. 5.32, the difference between the pressure p measured during the hysteresis study and the experimental model $p = p(u)$ equals about 1 kPa. This difference can be explained by a change of the ambient atmospheric pressure between the day when the experimental models were established and the day when the hysteresis loops were performed. This will be discussed later in more details.

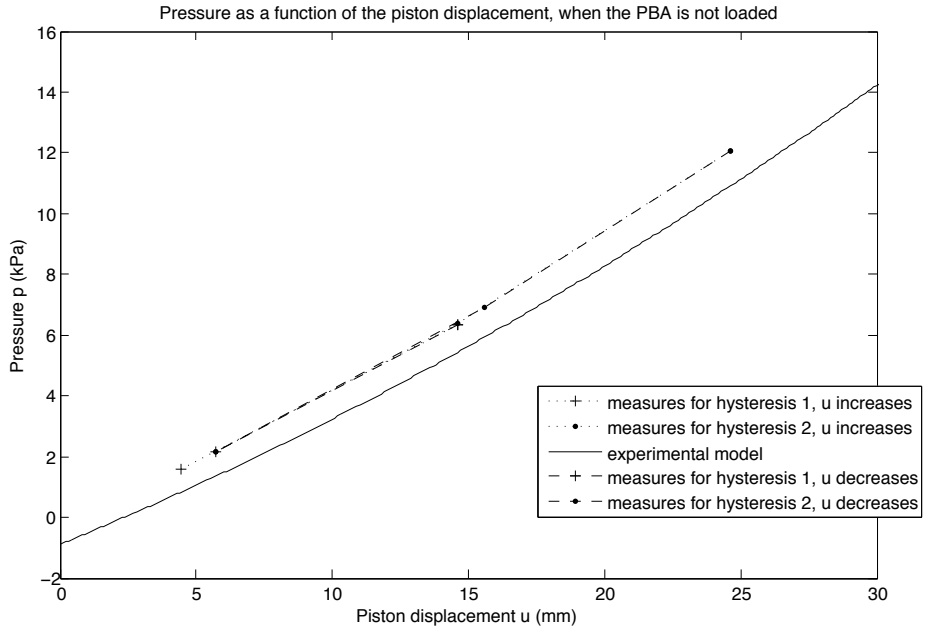

Figure 5.31: Hysteresis study of the pressure p with respect to the piston displacement u, when the PBA is not loaded: the test bench piston describes two cycles (one cycle = increasing phase of u + decreasing phase of u) during which p is measured. As can be seen, the pressure p presents nearly no hysteresis with respect to the piston displacement u.

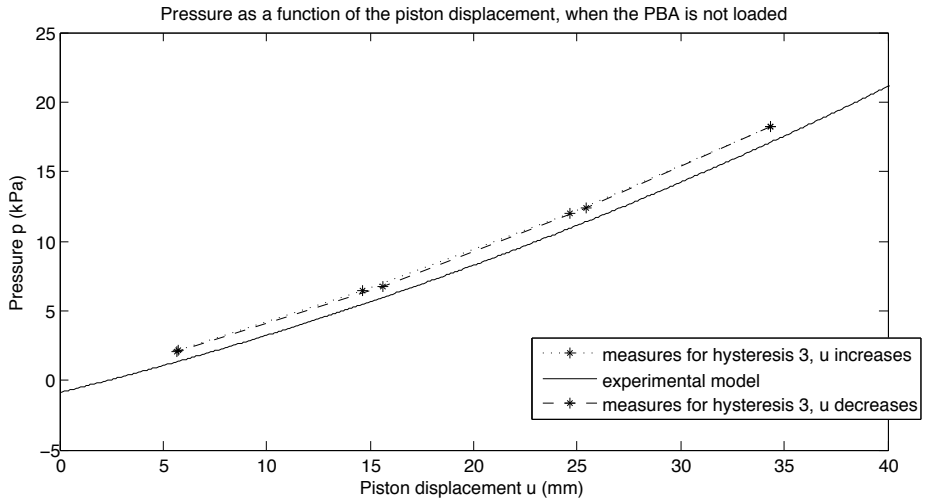

Figure 5.32: Hysteresis study of the pressure p with respect to the piston displacement u, when the PBA is not loaded: the test bench piston describes one cycle (one cycle = increasing phase of u + decreasing phase of u) during which p is measured. As can be seen, the pressure p presents nearly no hysteresis with respect to the piston displacement u.

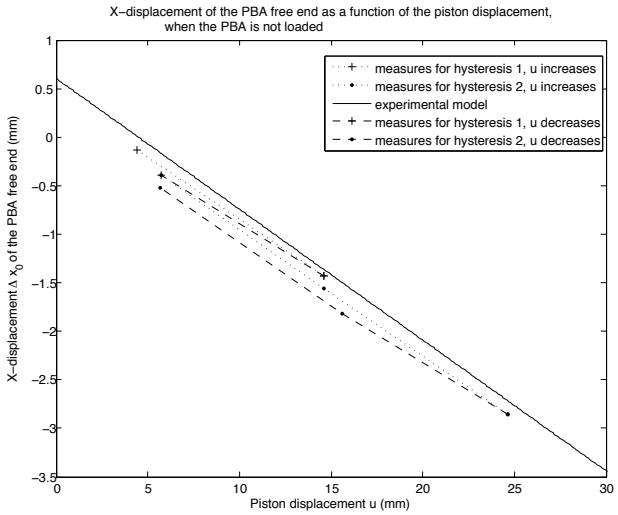

Figure 5.33: Hysteresis study of the X-displacement Δx_0 of the PBA free end with respect to the piston displacement u, when the PBA is not loaded: the test bench piston describes two cycles (one cycle = increasing phase of u + decreasing phase of u) during which Δx_0 is measured. As can be seen in the figure, it can be concluded that the X-displacement Δx_0 presents a hysteresis with respect to the piston displacement u: the maximum difference in X-displacement measured during the hysteresis loops is about 0.26 mm (the accuracy on the measurement of Δx_0 equals ± 0.13 mm).

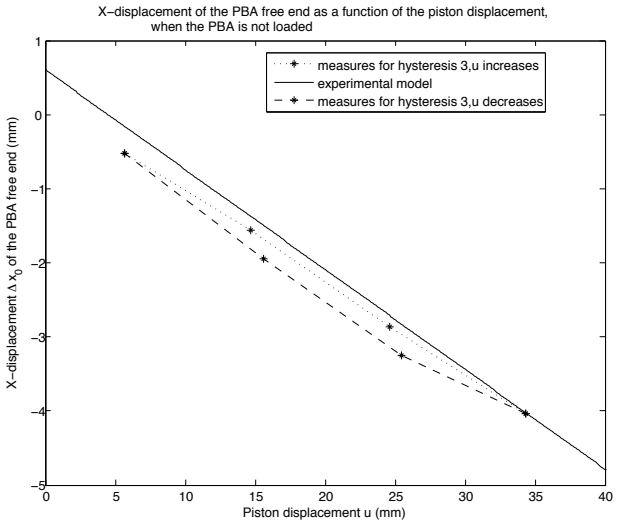

Figure 5.34: Hysteresis study of the X-displacement Δx_0 of the PBA free end with respect to the piston displacement u, when the PBA is not loaded: the test bench piston describes one cycle (one cycle = increasing phase of u + decreasing phase of u) during which Δx_0 is measured. As can be seen in the figure, it can be concluded that the X-displacement Δx_0 presents a hysteresis with respect to the piston displacement u: the maximum difference in X-displacement measured during the hysteresis loops is about 0.26 mm (the accuracy on the measurement of Δx_0 equals ± 0.13 mm).

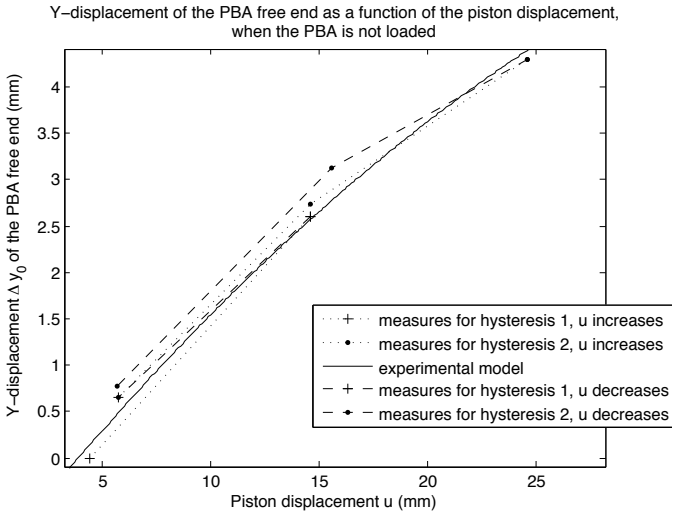

Figure 5.35: Hysteresis study of the Y-displacement Δy_0 of the PBA free end with respect to the piston displacement u, when the PBA is not loaded: the test bench piston describes two cycles (one cycle = increasing phase of u + decreasing phase of u) during which Δy_0 is measured. As can be seen in the figure, it can be concluded that the Y-displacement Δy_0 presents a hysteresis with respect to the piston displacement u: the maximum difference in Y-displacement measured during the hysteresis loops is larger than 0.26 mm (the accuracy on the measurement of Δy_0 equals ± 0.13 mm).

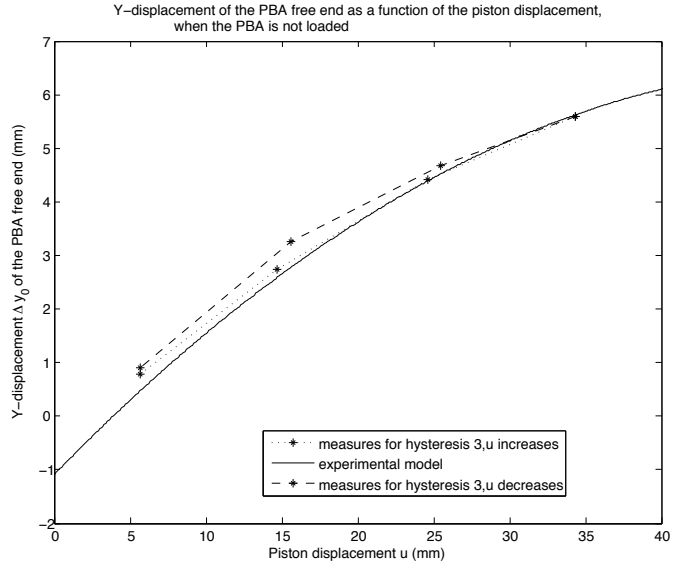

Figure 5.36: Hysteresis study of the Y-displacement Δy_0 of the PBA free end with respect to the piston displacement u, when the PBA is not loaded: the test bench piston describes one cycle (one cycle = increasing phase of u + decreasing phase of u) during which Δy_0 is measured. As can be seen in the figure, it can be concluded that the Y-displacement Δy_0 presents a hysteresis with respect to the piston displacement u: the maximum difference in Y-displacement measured during the hysteresis loops is larger than 0.26 mm (the accuracy on the measurement of Δy_0 equals ± 0.13 mm).

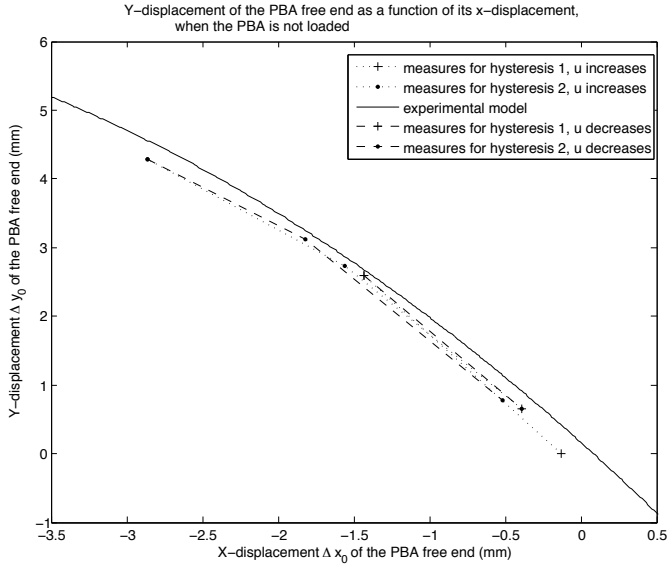

Figure 5.37: Hysteresis study of the X- and Y-displacements Δx_0 and Δy_0 of the PBA free end with respect to the piston displacement u, when the PBA is not loaded: the test bench piston describes two cycles (one cycle = increasing phase of u + decreasing phase of u) during which Δx_0 and Δy_0 are measured.

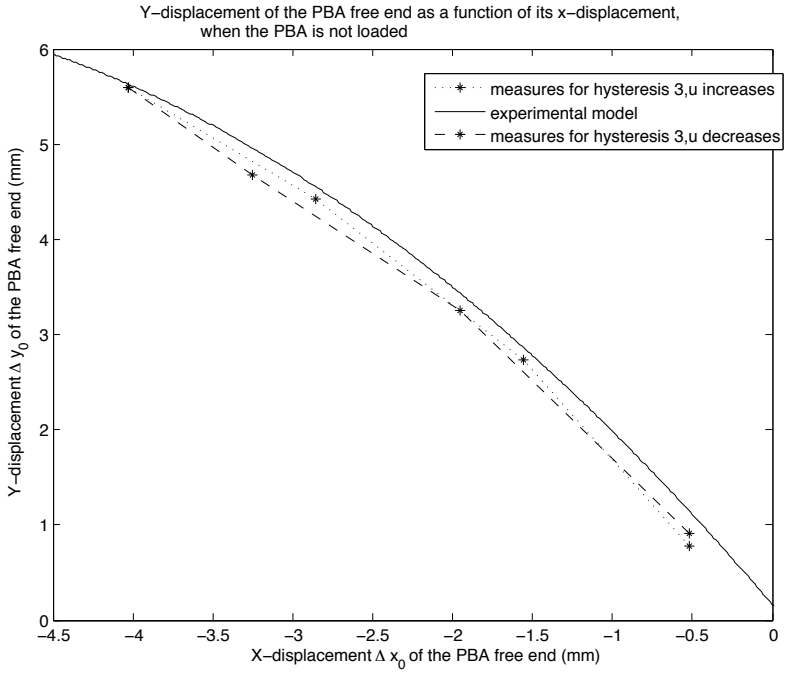

Figure 5.38: Hysteresis study of the X- and Y-displacements Δx_0 and Δy_0 of the PBA free end with respect to the piston displacement u, when the PBA is not loaded: the test bench piston describes one cycle (one cycle = increasing phase of u + decreasing phase of u) during which Δx_0 and Δy_0 are measured.

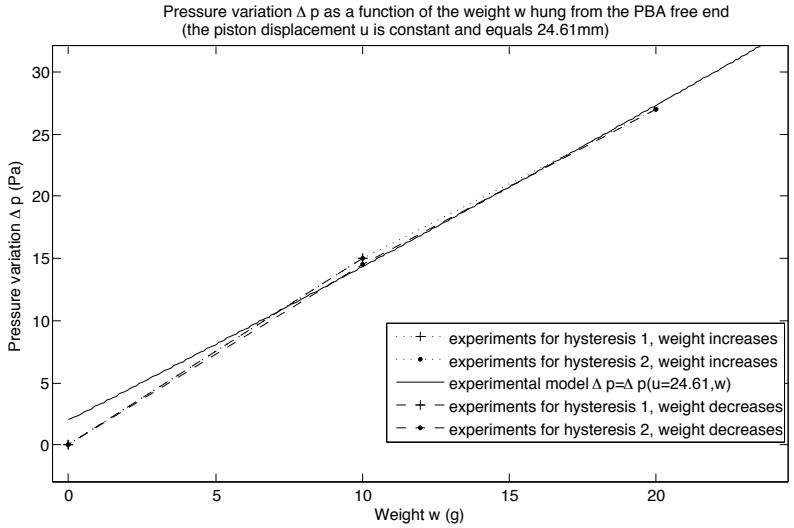

Figure 5.39: Hysteresis study of the pressure variation Δp with respect to the weight w hung from the PBA free end: the test bench piston is fixed at a given position $u = 24.61$ mm and two loading cycles of the PBA are performed (one cycle = increasing phase of w + decreasing phase of w) during which Δp is measured. As can be seen in the figure, it can be concluded that Δp presents nearly no hysteresis with respect to the weight w. Indeed, 0.5 Pa is the maximum difference in pressure variation measured during the hysteresis loops (the accuracy on a pressure variation measurement is $\leq \pm 4$ Pa).

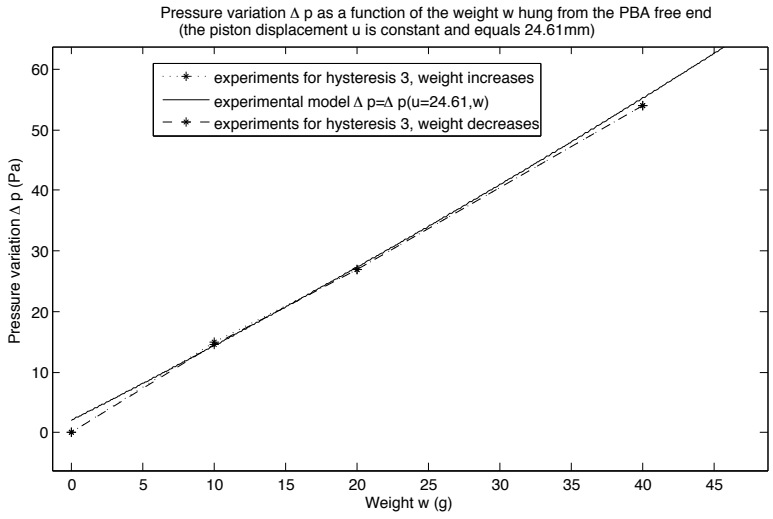

Figure 5.40: Hysteresis study of the pressure variation Δp with respect to the weight w hung from the PBA free end: the test bench piston is fixed at a given position $u = 24.61$ mm and one loading cycle of the PBA is performed (one cycle = increasing phase of w + decreasing phase of w) during which Δp is measured. As can be seen in the figure, it can be concluded that Δp presents nearly no hysteresis with respect to the weight w. Indeed, 0.5 Pa is the maximum difference in pressure variation measured during the hysteresis loops (the accuracy on a pressure variation measurement is $\leq \pm 4$ Pa).

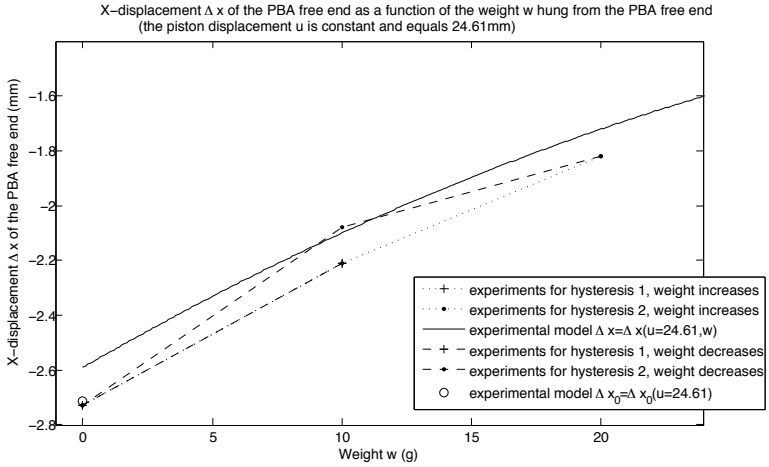

Figure 5.41: Hysteresis study of the X-displacement Δx of the PBA free end with respect to the weight w hung from the PBA free end: the test bench piston is fixed at a given position $u = 24.61$ mm and two loading cycles of the PBA are performed (one cycle = increasing phase of w + decreasing phase of w) during which Δx is measured. As can be seen in the figure, it can be concluded that Δx presents a hysteresis with respect to the weight w: the maximum difference in X-displacement measured during the hysteresis loops is smaller than 0.26 mm (the accuracy on the measurement of Δx equals ± 0.13 mm).

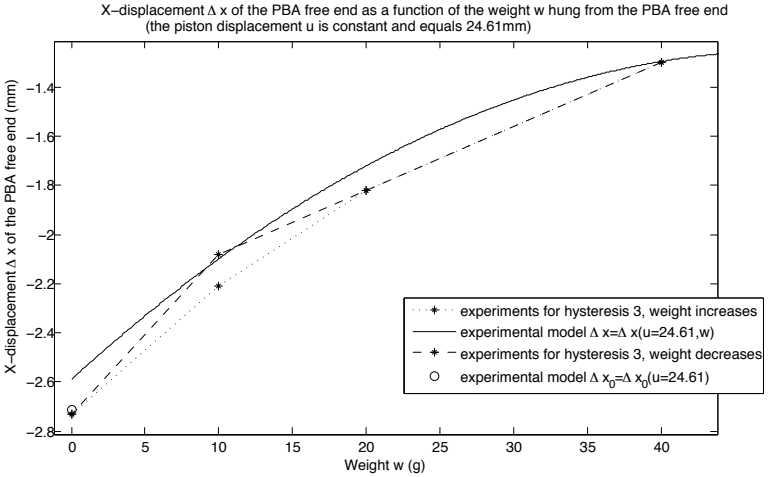

Figure 5.42: Hysteresis study of the X-displacement Δx of the PBA free end with respect to the weight w hung from the PBA free end: the test bench piston is fixed at a given position $u = 24.61$ mm and one loading cycle of the PBA is performed (one cycle = increasing phase of w + decreasing phase of w) during which Δx is measured. As can be seen in the figure, it can be concluded that Δx presents a hysteresis with respect to the weight w: the maximum difference in X-displacement measured during the hysteresis loops is smaller than 0.26 mm (the accuracy on the measurement of Δx equals ± 0.13 mm).

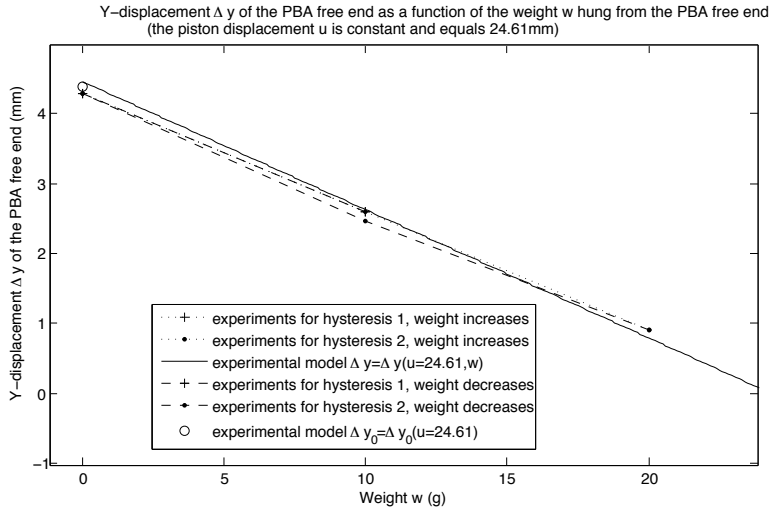

Figure 5.43: Hysteresis study of the Y-displacement Δy of the PBA free end with respect to the weight w hung from the PBA free end: the test bench piston is fixed at a given position $u = 24.61$ mm and two loading cycles of the PBA are performed (one cycle = increasing phase of w + decreasing phase of w) during which Δy is measured. As can be seen in the figure, it can be concluded that Δy presents a hysteresis with respect to the weight w: the maximum difference in Y-displacement measured during the hysteresis loops is smaller than 0.26 mm (the accuracy on the measurement of Δy equals ± 0.13 mm).

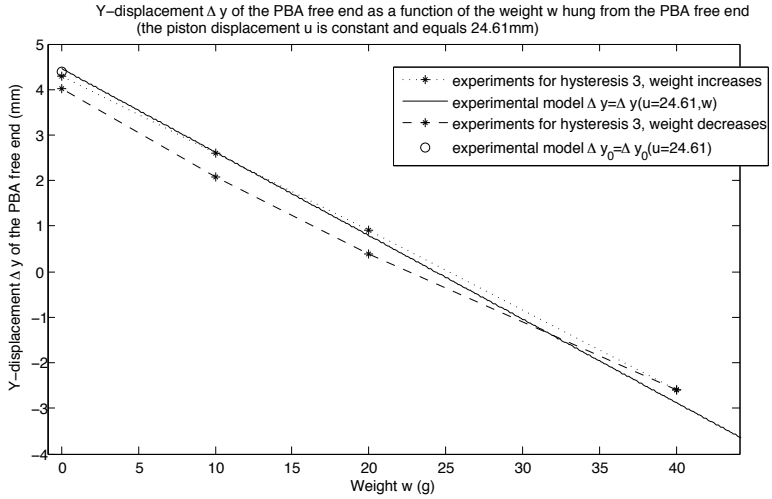

Figure 5.44: Hysteresis study of the Y-displacement Δy of the PBA free end with respect to the weight w hung from the PBA free end: the test bench piston is fixed at a given position $u = 24.61$ mm and one loading cycle of the PBA is performed (one cycle = increasing phase of w + decreasing phase of w) during which Δy is measured. As can be seen in the figure, it can be concluded that Δy presents a hysteresis with respect to the weight w: the maximum difference in Y-displacement measured during the third hysteresis loop is larger than 0.26 mm (the accuracy on the measurement of Δy equals ± 0.13 mm).

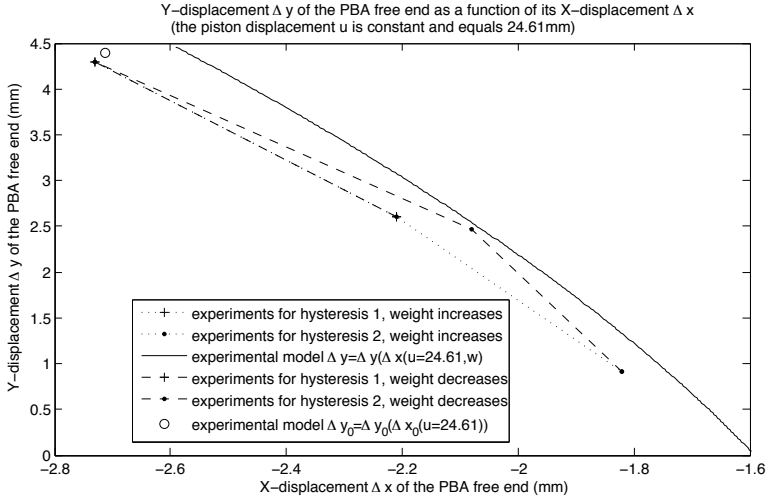

Figure 5.45: Hysteresis study of the X- and Y-displacements Δx and Δy of the PBA free end with respect to the weight w hung from the PBA free end: the test bench piston is fixed at a given position $u = 24.61$ mm and two loading cycles of the PBA are performed (one cycle = increasing phase of w + decreasing phase of w) during which Δx and Δy are measured.

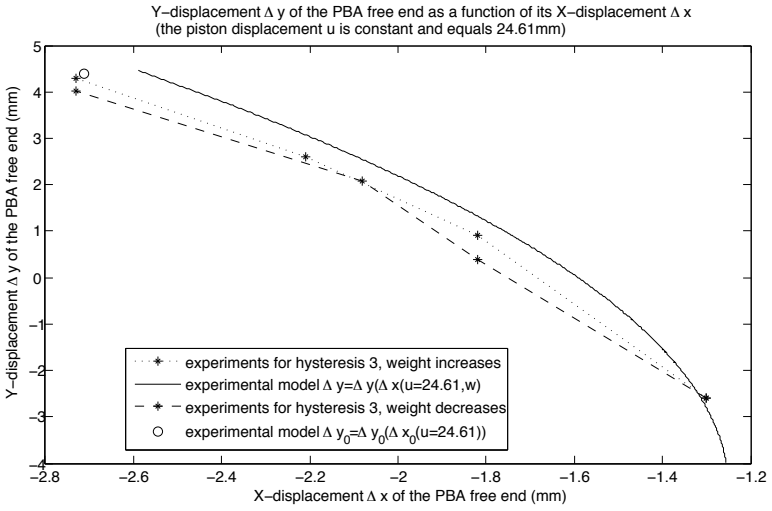

Figure 5.46: Hysteresis study of the X- and Y-displacements Δx and Δy of the PBA free end with respect to the weight w hung from the PBA free end: the test bench piston is fixed at a given position $u = 24.61$ mm and one loading cycle of the PBA is performed (one cycle = increasing phase of w + decreasing phase of w) during which Δx and Δy are measured.

5.3 Discussion

5.3.1 Relevance of the PVFP principle

Being able to determine the displacement of a flexible fluidic actuator and the force it develops thanks to the measurements of the fluid pressure and of the volume of the supplied fluid, means being able to determine the displacement and the force without a displacement sensor or a force sensor placed on the actuator [78].

This is an interesting measuring concept for applications where the space is limited and where a miniaturization effort is required. This is for example the case in Teleoperated Minimally Invasive Surgery (MIS), where it is necessary to measure the force applied by the tools to the organs to ensure a force feedback of good quality. However, this measurement is not straightforward. Indeed, if the force sensor is placed outside the body of the patient, the measurement will be polluted by the friction of the trocar. To solve this problem, some researchers propose to place the sensor at the end of the tool but this raises the challenge to develop a small and sterilizable force sensor [63]. Using flexible fluidic actuators to actuate the surgical tools would allow to measure the force applied to the organs without the need of a force sensor. Besides, flexible fluidic actuators could also answer the need for flexible instruments, i.e. instruments presenting a large number of DOFs and able to perform snake-like movements when avoiding obstacles. This need has been expressed by the medical field in applications such as the MIS [33], the endoluminal surgery [4] or the active catheters [45].

In [52], a flexible sensor to be placed under the PBA is proposed. It is a flexible plate presenting a pneumatic channel. Airflow is supplied to the channel and the bending of the PBA is detected by measuring the airflow changes in the channel. Besides, measuring the airflow changes in the channel and the pressure inside the PBA allows to determine the stiffness of an object in contact with the PBA. If the PVFP principle was implemented on this PBA, it would allow doing the same measurements without such an additional sensor. Indeed, a piston displacement u could be performed so that the PBA bends and comes in contact with the object to palpate. The PVFP principle allows then to determine the contact force F between the PBA and the object and the displacement Δz the PBA has performed while pushing on the object. These two informations can then be used to determine the stiffness $F/\Delta z$ of the object.

The PVFP principle has been experimentally validated with the PBA, i.e. an actuator presenting only one DOF. With such an actuator, the applied force can be predicted at only one precise point and along only one precise direction. However, the principle could be applied to more complex structures. For example, let us consider the "Flexible Microactuator" described in [78] (see Fig. 5.47). It is a cylinder whose end is closed and which presents three internal chambers. It is composed of silicone rubber reinforced with nylon fibres disposed in a circular direction. The function of these fibres is to prevent radial deformations. When one chamber is pressurized, the cylinder bends in the direction opposite this chamber. This actuator presents three DOFs (one stretching and two bending motions). Measuring the pressure in the three chambers and the fluid volume supplied to the chambers would allow to determine the posture of the actuator and the three components of any force applied to a precise given point, for example, to the end point of the actuator.

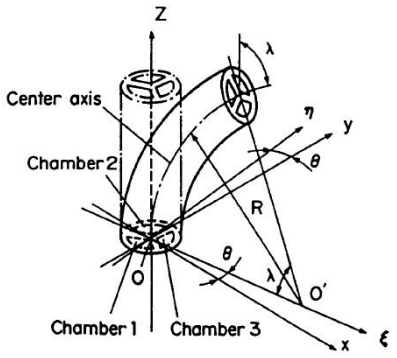

Figure 5.47: Bending Flexible Microactuator (FMA): when a chamber is pressurized, its length increases while the other chambers keep their initial length and consequently the cylinder bends in the direction opposite the pressurized chamber. The figure presents a bending FMA whose chambers no. 1 and 2 are pressurized. Figure from [72].

5.3.2 Practical implementation of the PVFP principle in a targeted application

As can be seen in Fig. 5.26 and 5.27, for a given piston displacement u, there exists a duality between the force developed by the PBA free end (or in other words, the weight attached to its end) and the displacements Δx and Δy of its tip: if the load of the PBA increases, the PBA free end moves downwards and the displacements Δx and Δy decrease in absolute value. It is thus not possible to impose the displacements of the PBA tip and the force it develops at the same time. In practical applications, a choice will have to be made between imposing the force and imposing the displacements, according to the task to be performed.

The PVFP principle could be implemented in a control loop in order to control the displacement of a flexible fluidic actuator tip or the force it develops, without using displacement or force sensor. If the dynamics of the system are quite slow, static models such as those established for the PBA in this chapter can be used in the control loop. Hence, the control loop makes a quasi-static approximation of the system dynamics. For example, to control the actuator displacement, the control loop presented in Fig. 5.48 can be build. It works as follows:

1. The actuator is required to perform a displacement Δy^*.

2. Δy^* is compared to the predicted displacement Δy.

3. The difference $\Delta y^* - \Delta y$ is the input of the model of the flexible fluidic actuator. Knowing the value of the predicted external force F_{ext} applied to the actuator, the model determines the piston displacement u^* that needs to be performed in order to reach Δy^*.

4. u^* is compared to the actual measured piston displacement u and the difference $u^* - u$ is the input of a controller. It acts on the physical system so that the required piston displacement is achieved. The physical system comprises the flexible fluidic actuator and the syringe-pump pressurization system.

5. The piston displacement u and the pressure p are measured on the physical system.

6. On the basis of the measurements u and p, the model of the flexible fluidic actuator predicts the displacement Δy performed by the actuator and the external force F_{ext} applied to the actuator. These predictions are then used as if they were measurements.

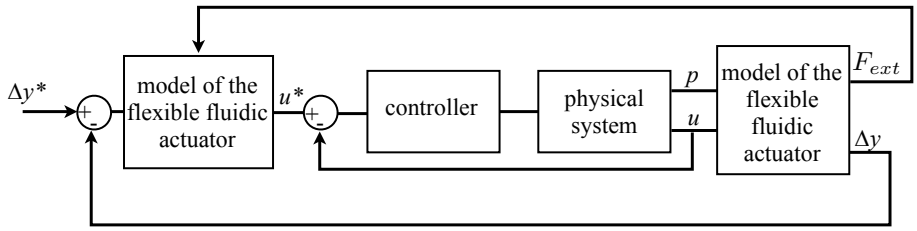

Figure 5.48: Control loop in which the PVFP principle is implemented in order to control the displacement Δy of the flexible fluidic actuator, without using force or displacement sensors.

The quality of the predictions provided by the PVFP principle implemented on the flexible fluidic actuator has to be evaluated with respect to the targeted application. Indeed, the predictions can be accurate enough for a given application but not for another one.
The same remark can be made if the actuator presents hysteresis. Before modeling the hysteresis, it has to be assessed whether this hysteresis is problematic or not with respect to the targeted application. Indeed, for a given application, the hysteresis may be small enough to be negligible; in this case, there is no need to model the hysteresis. On the other hand, for another application, the same hysteresis may be too large to be ignored; in this case, it has to be modeled properly.

The practical implementation of the PVFP principle raises some questions such as the effect that a variation of the ambient atmospheric pressure or temperature would have on the predictions provided by the PVFP principle. This question has already been discussed in Section 5.1.1 in the case of a simple flexible fluidic actuator but it would be interesting to try answering this question in the case of the PBA studied here. Fig. 5.49 presents a schematic view of the PBA linked to the cylinder of the test bench. The actuation fluid is air but the PVFP principle should also work with an incompressible fluid. Maybe a difference happens when a weight is hung from the PBA free end: since the volume in the cylinder will not change because the piston position is fixed, the volume of the PBA will not change and the position of the PBA free end will remain the same. On the other hand, it is also possible, thanks to the elasticity of the PBA rubber that the PBA free end moves downwards while the PBA keeps the same volume.

First, let us consider a change of the atmospheric pressure or ambient temperature happening when using the PBA and the PVFP principle implemented on it:

1. The actuation fluid is incompressible:

   - If the atmospheric pressure increases by an amount p^*, the absolute outside pressure p_{out} increases by the same amount. The volume of the PBA does not change because the volume of fluid inside the cylinder does not change and since the atmospheric pressure is applied to the top of the PBA as well as on its underside, the atmospheric pressure increase will not modify the displacements of point A. Since the shape of the PBA does not change, the inner absolute pressure p_{in} will probably increase by the same amount as p_{out} and the PVFP principle implemented on the actuator perceives this as the application of a load w^* that would have decreased the displacement of the PBA free end. The predictions of the PVFP

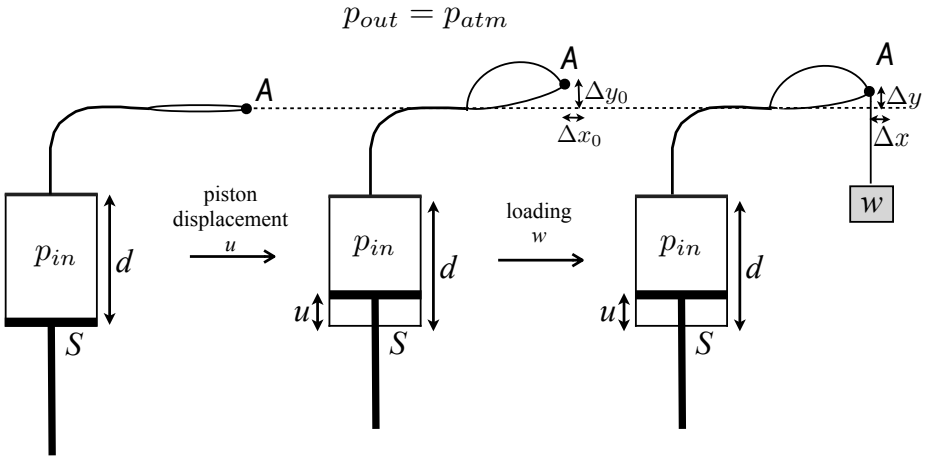

Figure 5.49: Pneumatic Balloon Actuator (PBA) linked to the cylinder of the test bench. The actuation fluid is air. When a displacement u is imposed to the piston, the inner pressure p_{in} increases and the PBA inflates and its free end A moves upwards. The vertical and horizontal displacements of this point are Δy_0 and Δx_0, respectively. Afterwards, keeping the piston position constant, if a weight w is hung from the PBA free end, the inner pressure p_{in} increases and the displacements Δy and Δx of the PBA free end decrease. According to the PVFP principle, knowing the values of p_{in} and u allows to determine the displacements of point A and the value of the weight w.

principle are distorted but to get rid of the influence of an atmospheric pressure change, a gauge pressure sensor could be used to measure p_{in} (it was the case for the experiments performed on the PBA in this chapter) or the atmospheric pressure could be measured so that the false prediction of the PVFP principle can be corrected.

- If the ambient temperature increases by a small amount such that the volume of fluid does not change (no expansion), it will have no influence on the results provided by the PVFP principle, i.e. the predictions of the actuator displacement and of the external pressure applied to the membrane will not be distorted.

2. The actuation fluid is compressible.

   - If the atmospheric pressure increases by an amount p^*, the absolute outside pressure p_{out} increases by the same amount, the volume of the PBA decreases and point A moves downwards. p_{in} increases but probably not by the same amount as p_{out}. The PVFP principle implemented on the actuator perceives the change of the atmospheric pressure as the application of a load w^* that would have decreased the vertical displacement of point A. However, it is not sure that using this prediction would allow to compensate correctly the change of the displacements of point A. The PVFP principle does not allow to distinguish a change of the atmospheric pressure from the application of a load to the PBA free end; to be able to do so, it is necessary to measure the atmospheric pressure.
   - If the ambient temperature increases, the volume of fluid expands in the actuator. Since the volume V' in the cylinder does not change because the piston position is imposed, the volume of the PBA increases and point A moves upwards. The inner pressure p_{in} increases and the PVFP principle implemented on the actuator perceives this change as the application of a load $w*$ that would have decreased

the vertical displacement of point A. Hence, the prediction of the PVFP principle can not be used to compensate the change of displacements of point A due to the temperature increase; indeed, doing so would lead to a further increase of the displacement of this point! The temperature needs thus to be measured and taken into account in the implementation of the PVFP principle and its effect on the PBA free end displacement needs to be compensated.

In conclusion, the PVFP principle seems applicable to the PBA with an incompressible or a compressible actuation fluid. Besides, if the PVFP principle is implemented on the PBA with an incompressible fluid and a gauge pressure to measure p_{in}, it seems that the predictions provided by the PVFP principle implemented on the actuator will not be influenced by the changes of the atmospheric pressure and of the temperature, occuring during the use of the actuator.

During the experiments described in this chapter, the actuation fluid that has been used is air. Since the fluidic circuit presents some leakages, it is refilled with air at atmospheric pressure before each use of the test bench. A change of atmospheric pressure or ambient temperature can then happen between the day when the models were established and the day when the test bench is used again and refilled with air, whose initial pressure or temperature has thus changed.
During the use of the PBA, the quantity of gas is constant and if the temperature is constant, the gas law leads to the following equation:

$$\frac{p_{atm}Sd}{T} = \frac{p_{in}(V_{PBA} + S(d-u))}{T} \tag{5.25}$$

As can be seen, if the temperature is constant during the use of the actuator, it has no effect on the equation. Hence, if the ambient temperature was $T = T_1$ the day when the experimental models have been established and $T = T_2$ the day when the test bench has been refilled with air, the difference between T_1 and T_2 will have no influence on equation (5.25) and the experimental models on which the PVFP rests will still be valid.
If the atmospheric pressure was $p_{atm} = p_{atm\_1}$ the day when the experimental models have been established and $p_{atm} = p_{atm\_2}$ the day when the test bench has been refilled with air, the experimental models on which the PVFP rests will no more be valid due to the difference between p_{atm_1} and p_{atm_2} and its influence on equation (5.25). This is what happened with the hysteresis studies presented in Section 5.2.3. Since equation (5.25) had changed, the relationship between p_{in} and u changed also, as can be seen in Fig. 5.31 and 5.32 when the PBA was not loaded.
Again, with an incompressible fluid, such a change of the atmospheric pressure seems to have no influence on the PVFP principle, if a gauge pressure is used or if the atmospheric pressure is monitored.

As explained in Section 5.1 and above for the PBA, the PVFP principle seems to work for those flexible fluidic actuators whatever the actuation fluid (compressible or incompressible). Hence, for medical applications where gas leakages are forbidden, the PVFP principle can be implemented on these flexible fluidic actuators actuated by an incompressible physiological saline solution.

Replacing gas by liquid brings also the advantage that the system gets rid of the compressibility of the actuation fluid. During the experiments presented in this chapter, it has been noticed that the gas pressure takes several minutes to stabilize after a piston displacement. This can be seen in Fig. 5.50 when the piston displacement decreases from $u = 34.35$ mm to $u = 5.7$ mm. As can be noticed, the pressure decreases until a minimum value and then

slightly increases to reach a stabilized value after approximately 3 minutes (the stabilization of the pressure can not be seen in the figure).
Fig. 5.51 presents what happens if the piston displacement increases from $u = 5.7$ mm to $u = 34.36$ mm. As can be seen, the pressure increases until a maximum value and then decreases slightly to reach a stabilized value after approximately 4.3 minutes (the stabilization of the pressure can not be seen in the figure).
The fact that the pressure needs a long time to stabilize can be accredited to the gas compressibility, to the elasticity of the pneumatic tubes and to the elasticity of the flexible fluidic actuator. Studying the quantitative effect of each of these three causes would help to determine which action to take in order to reduce the establishment time of the pressure in the fluidic circuit and to increase the bandwidth of the system.
However, before performing this study, it would be interesting to study the sensibility of the actuator displacements with regard to the pressure establishment. Indeed, as can be seen in Fig. 5.50 and 5.51, in the case of the test bench used in this chapter, when the pressure establishes itself, its variation is of maximum 1 kPa. If this variation has a small effect on the actuator displacements, it may be superfluous to make a thorough study of the pressure dynamics.
Remark: In the experiments described in this chapter, the measurements have been made once the pressure had stabilized.

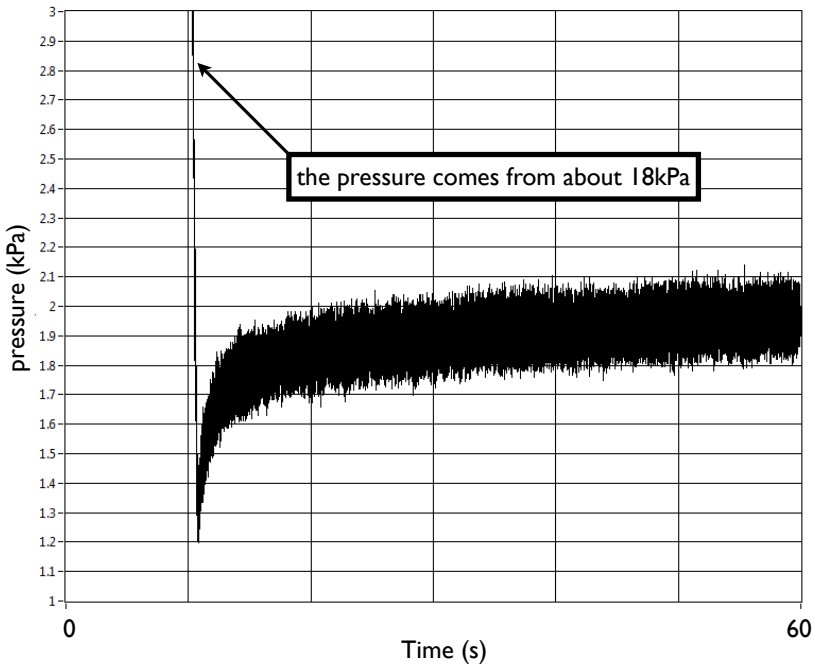

Figure 5.50: Evolution of the pressure in the test bench fluidic circuit when the piston displacements decreases from $u = 34.35$ mm to $u = 5.7$ mm.

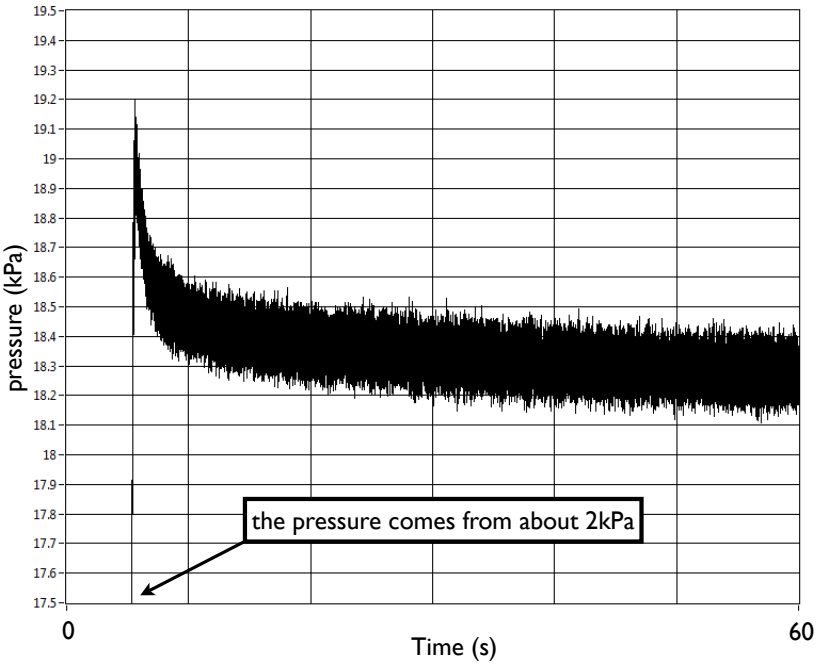

Figure 5.51: Evolution of the pressure in the test bench fluidic circuit when the piston displacement increases from $u = 5.7$ mm to $u = 34.36$ mm.

However, replacing gas by liquid implies larger pressure losses whose effect has to be studied. Besides, a flexible fluidic actuator filled with liquid will be heavier and as a consequence it will develop smaller displacements, for a given pressure level, than the same actuator filled with gas. Hence, the actuator will probably present a pressure threshold because a minimum pressure level will be required to compensate the weight of the liquid. An actuator filled with liquid will also be less compliant.